JHEP

Published for SISSA by Springer

Received: June 25, 2015
Accepted: October 17, 2015
Published: November 10, 2015

Heavy baryons as polarimeters at colliders

Mario Galanti,[a] **Andrea Giammanco,**[b,c] **Yuval Grossman,**[d] **Yevgeny Kats,**[e] **Emmanuel Stamou**[e] **and Jure Zupan**[f]

[a] *Department of Physics and Astronomy, University of Rochester, Rochester, NY 14627-0171, U.S.A.*

[b] *Centre for Cosmology, Particle Physics and Phenomenology, Université catholique de Louvain, B-1348 Louvain-la-Neuve, Belgium*

[c] *National Institute of Chemical Physics and Biophysics, 10143 Tallinn, Estonia*

[d] *Laboratory for Elementary-Particle Physics, Cornell University, Ithaca, NY 14853, U.S.A.*

[e] *Department of Particle Physics and Astrophysics, Weizmann Institute of Science, Rehovot 7610001, Israel*

[f] *Department of Physics, University of Cincinnati, Cincinnati, OH 45221, U.S.A.*

E-mail: mario.galanti@cern.ch, andrea.giammanco@uclouvain.be, yg73@cornell.edu, yevgeny.kats@weizmann.ac.il, emmanuel.stamou@weizmann.ac.il, zupanje@ucmail.uc.edu

Abstract: In new-physics processes that produce b or c jets, a measurement of the initial b or c-quark polarization could provide crucial information about the structure of the new physics. In the heavy-quark limit, the b and c-quark polarizations are preserved in the lightest baryons they hadronize into, Λ_b and Λ_c, respectively. We revisit the prediction for the polarization retention after the hadronization process and extend it to the case of transverse polarization. We show how ATLAS and CMS can measure the b-quark polarization using semileptonic Λ_b decays, and the c-quark polarization using $\Lambda_c^+ \to pK^-\pi^+$ decays. For calibrating both measurements we suggest to use $t\bar{t}$ samples in which these polarizations can be measured with precision of order 10% using 100 fb^{-1} of data in Run 2 of the LHC. Measurements of the transverse polarization in QCD events at ATLAS, CMS and LHCb are motivated as well. The proposed measurements give access to nonperturbative QCD parameters relevant to the dynamics of the hadronization process.

Keywords: QCD Phenomenology, Hadronic Colliders

ArXiv ePrint: 1505.02771

doi:10.1007/JHEP11(2015)067

JHEP11(2015)067

Contents

JHEP11(2015)067

1 Introduction

In order to fully explore the nature of new particles, both the sizes and the Lorentz structures of their couplings will need to be measured. Probing the Lorentz structure is particularly challenging as it often requires measuring the polarizations of final-state particles. Information about the polarization of colored decay products is typically washed away by hadronization. A well-known exception is the top quark [1, 2], which decays before it hadronizes. In this paper we show that, while challenging, the polarization of b and c quarks can also be measured at the LHC, despite hadronization.

Knowing how to extract the b-quark polarization could facilitate a variety of interesting measurements. For instance, in $h \to b\bar{b}$ decays one could examine whether the Higgs coupling to b quarks has a CP-violating component, $h\bar{b}\gamma^5 b$, in analogy to the $h \to \tau^+\tau^-$ case [3]. Similarly, if a stop or a sbottom is discovered and its decay produces b's, one could determine whether it is the left-handed or the right-handed one, or, more generally, determine the left-right mixing angle. Also c quarks play an important role in a variety of new-physics scenarios, e.g. refs. [4–8].

As a proxy for the b-quark polarization we are proposing to use the Λ_b polarization. The Λ_b is a spin-1/2 baryon, which is produced in b-quark hadronization both directly and from the decays of Σ_b and Σ_b^* baryons, in comparable amounts. The main point is that, in contrast to the B mesons, the Λ_b is expected to retain the polarization of the b quark to a high degree, at least in the heavy-quark limit [9–11]. About one out of ten b quarks produces a Λ_b, and these events can be used for extracting the b-quark polarization.

We define the fraction of polarization retained in hadronization to a Λ_b as

$$r_{\hat{\mathcal{P}}} \equiv \frac{\mathcal{P}(\Lambda_b)}{\mathcal{P}(b)}\,, \tag{1.1}$$

where $\mathcal{P}(b)$ is the polarization of the b quark as it exits the hard process and $\mathcal{P}(\Lambda_b)$ is the Λ_b polarization when it decays. In general, $r_{\hat{\mathcal{P}}}$ depends on the initial polarization direction, $\hat{\mathcal{P}}(b)$. If the b is either longitudinally or transversely polarized, then $r_{\hat{\mathcal{P}}}$ is a number, r_L or r_T, respectively, while it is a tensor in general. In the heavy-quark limit, $m_b \gg \Lambda_{\rm QCD}$, one has $r_{\hat{\mathcal{P}}} = 1$. For the physical b mass we thus expect $r_{\hat{\mathcal{P}}}$ to be $\mathcal{O}(1)$ [9–11], where the precise number depends on relatively uncertain hadronization parameters. We suggest to measure $r_{\hat{\mathcal{P}}}$ at the LHC in Standard Model (SM) processes with polarized b quarks. The results will allow interpreting similar future measurements of b-quark polarization in new-physics processes.

As long as the hard scale, Q, at which the b quarks are produced is much larger than the QCD scale, $Q \gg \Lambda_{\rm QCD}$, the b-quark hadronization and the subsequent evolution factorize from the short-distance production process. Therefore $r_{\hat{\mathcal{P}}}$ is a universal quantity, independent of the exact mechanism that produces the initial b quark. In general, $r_{\hat{\mathcal{P}}}$ depends on the scale, Q, and the fraction of the b-quark momentum carried by the Λ_b, z. The important point is that once we know $r_{\hat{\mathcal{P}}}(z)$ at a given scale, we can calculate it at a different scale using the known renormalization group (RG) evolution of fragmentation functions. A measurement of $r_{\hat{\mathcal{P}}}(z)$ using a SM process at some scale Q will then enable us to know $r_{\hat{\mathcal{P}}}(z)$ at any scale and use it in new-physics measurements. Moreover, the effects

JHEP11(2015)067

of scale dependence are small as long as the characteristic scales of the measurements are similar. Thus, at the first stage, measurements inclusive in z are sufficient. Only once we enter a precision era will one need to take into account the effects of running.

Depolarization occurs both during and after hadronization. During hadronization the flip of the b-quark spin occurs via QCD-scale processes. It is $\Lambda_{\rm QCD}/m_b$ suppressed because the b-quark chromomagnetic moment is $\mu_b \propto 1/m_b$ and is, as such, small. After hadronization, depolarization occurs mainly because Λ_b's are also produced from $\Sigma_b^{(*)}$ decays whose lifetimes are longer than the timescale for hadronization into distinct mass eigenstates Σ_b and Σ_b^*, i.e., $\Gamma_{\Sigma_b^{(*)}} < m_{\Sigma_b^*} - m_{\Sigma_b}$. Even though this effect vanishes in the formal $m_b \to \infty$ limit, it is $\mathcal{O}(1)$ for the physical b-quark mass [11]. The dominant depolarization effect is therefore due to the $\Sigma_b^{(*)}$ decays.

Evidence for longitudinal Λ_b polarization in $Z \to b\bar{b}$ decays has already been seen at LEP [12–14], but precise measurements of r_L were impossible. At the LHC, the $Z \to b\bar{b}$ sample suffers from a large QCD background, $pp \to b\bar{b} + X$ [15], which makes the measurement difficult despite the fact that the background b's are only slightly (and just transversely) polarized. In contrast, as we demonstrate in this paper, the b's from top-quark decays at the LHC allow for a clean measurement of r_L at ATLAS and CMS with the upcoming Run 2 datasets.

It would also be useful to measure r_T using the transverse polarization of b's produced in QCD events. The polarization in QCD events arises at NLO and for large momenta behaves like $\mathcal{P}(b) \sim \alpha_s m_b/p_b$, where p_b is the b-quark momentum [16]. Since it is larger for softer b quarks, the corresponding Λ_b decays are probably easiest to reconstruct at LHCb (although to use Λ_b as a b-quark proxy, the b quarks still need to be hard enough for factorization to apply). However, the polarization varies significantly as a function of the parton-level kinematics of the event, and even changes its sign for some of the contributing processes [16]. The limited angular coverage of LHCb may hinder using this kinematic dependence, which is ignored in the existing LHCb measurement [17]. Therefore, low-p_T measurements by ATLAS and CMS, e.g. along the lines of refs. [18, 19], seem to be motivated as well.

An additional motivation for measuring the Λ_b polarization (and a few related quantities, as we will discuss) in SM processes is that it can teach us a lot about the hadronization process and provide access to several nonperturbative QCD parameters. As we will review, the present knowledge of the relevant physics is incomplete. The results of the measurements can also be useful in tuning Monte Carlo generators.

In the case of c quarks, the physics of the relevant baryons (Λ_c, $\Sigma_c^{(*)}$) is qualitatively similar to the b-quark case. It is likely that an $\mathcal{O}(1)$ fraction of the polarization is preserved despite the fact that $m_c \gg \Lambda_{\rm QCD}$ is not a very good assumption. The transverse polarization of Λ_c's from QCD production has already been seen in the fixed-target experiments NA32 [20] and E791 [21], but theoretical interpretation is difficult because soft QCD effects may play a major role for the relatively low Λ_c momenta probed in these experiments. We will discuss how r_L can be measured at ATLAS and CMS using a $t\bar{t}$ sample, in which polarized c quarks are available from $W^+ \to c\bar{s}$ decays.

JHEP11(2015)067

The rest of the paper is organized as follows. In section 2 we describe the basic properties of the baryons of interest, while in section 3 (and appendices A and B) we study the polarization transfer from the heavy quark to the baryon. In sections 4 and 5 we analyze how to measure the polarization of the relevant b or c baryons at the LHC and propose specific analyses for such measurements in $pp \to t\bar{t}$. In section 6 we discuss how to obtain additional information by studying $\Sigma_b^{(*)}$, $\Sigma_c^{(*)}$ contributions in isolation. We summarize in section 7. Appendix C describes the relation between $r_{\hat{\mathcal{P}}}$ and fragmentation functions.

2 Bottom and charmed baryons

A b quark can combine with a light diquark[1] to produce a baryon. Most commonly, the diquark is made out of u and/or d quarks, producing either the isosinglet spin-1/2 baryon, Λ_b, or one of the isotriplet spin-1/2 or spin-3/2 baryons, Σ_b and Σ_b^*, respectively. The latter decay primarily through QCD as $\Sigma_b^{(*)} \to \Lambda_b \pi$, while $\Sigma_b^* \to \Sigma_b$ decays can be neglected. The Λ_b decays via weak interactions and can be treated as an asymptotic state in our discussion.

The probability for a b quark to fragment into any baryon is

$$f_{\text{baryon}} = (8.0 \pm 1.0)\,\%\,, \tag{2.1}$$

based on LEP measurements of $Z \to b\bar{b}$ decays as summarized in table 5 of ref. [23]. This number includes $f_{\text{baryon}} = f_{\Lambda_b} + f_{\Xi_b} + f_{\Omega_b}$, where Ξ_b and Ω_b are baryons that contain one and two strange quarks, respectively. Baryons that decay to Λ_b before the b itself decays, such as $\Sigma_b^{(*)}$, are included in f_{Λ_b} (and similarly for f_{Ξ_b} and f_{Ω_b}). We estimate the Λ_b contribution to f_{baryon} to be about 85% [24, 25], while the rest is primarily Ξ_b, which is studied in appendix B. This estimate is obtained from the relative rates of the $b \to \Lambda_b \to J/\psi\,\Lambda$, $b \to \Xi_b^- \to J/\psi\,\Xi^-$, $b \to \Omega_b^- \to J/\psi\,\Omega^-$ processes measured in QCD events at the Tevatron [24], using theoretical predictions for the branching ratios to J/ψ [25], and assuming $f_{\Xi_b^0} = f_{\Xi_b^-}$. For numerical estimates in the rest of the paper we will therefore use

$$f_{\Lambda_b} = 7\%\,. \tag{2.2}$$

In the near future, the LHC experiments will likely shed more light on the baryon fragmentation fractions.

The c quark has a similar spectrum of baryon states. The fragmentation fraction of a c quark into a Λ_c, based on LEP measurements [26], is

$$f_{\Lambda_c} = (5.7 \pm 0.7)\,\%\,. \tag{2.3}$$

Several experiments reported that in QCD events f_{Λ_b} varies significantly as a function of the b-hadron p_T, even for $p_T \gg \Lambda_{\text{QCD}}$, where factorization is expected to hold [23, 27–30]. This should *not* be interpreted as a variation of f_{Λ_b} from eq. (2.2) with the energy scale of the process. Events with the same p_T of Λ_b can come from b jets with very different p_T of the original b quark, by which we mean the total p_T of the b jet, after adding the

[1] The concept of a diquark, as the state of the light degrees of freedom within a heavy baryon, has precise meaning in the framework of the Heavy Quark Effective Theory (HQET). For a review, see, e.g., ref. [22].

JHEP11(2015)067

reconstructed neutrino p_T if relevant. One gets contributions from b jets where the Λ_b carries most of the b-quark momentum as well as from much harder b jets where the Λ_b carries only part of the momentum. Because the QCD production cross section changes rapidly with the b-quark p_T, a small difference in the shapes of the fragmentation functions of different b hadrons can translate into a large difference in their contributions to fixed hadron-p_T bins (see also ref. [31]). This can lead to an apparent p_T dependence of the fragmentation fractions even if it is absent at the fundamental level. As discussed in more detail in appendix C, a much clearer interpretation would be obtained if the measurements were performed in terms of fixed reconstructed b-quark p_T rather than b-hadron p_T. In that case one expects to see only a slow (logarithmic) dependence on the hard scale due to RG evolution. That is, it would be desirable for the LHC experiments to perform measurements of the differential cross sections $d\sigma/dp_T$ in terms of the reconstructed b-quark p_T. When enough data are available one should also perform measurements of $d^2\sigma/dp_T dz$, where z is the Λ_b momentum fraction relative to the initial p_T of the b quark.

As mentioned above, the Λ_b polarization carries information about the initial b-quark polarization and the leading depolarization effects are due to Σ_b and Σ_b^* decays. To describe the relative production probabilities of Λ_b, Σ_b, and Σ_b^*, we write their wave functions in terms of diquark and b-quark states. The diquark can be a spin singlet, S, or a spin triplet, T. This allows for four possible spin configurations, $S_0\,, T_{+1}\,, T_0\,, T_{-1}$, where the subscripts denote the spin projection along the spin-quantization axis. Using the same quantization axis for the spin of the b quark, the baryon mass eigenstates are

$$|\Lambda_{b,\pm\frac{1}{2}}\rangle = |b_{\pm\frac{1}{2}}\rangle|S_0\rangle\,, \tag{2.4}$$

$$|\Sigma_{b,\pm\frac{1}{2}}\rangle = \mp\sqrt{\frac{1}{3}}\,|b_{\pm\frac{1}{2}}\rangle|T_0\rangle \pm \sqrt{\frac{2}{3}}\,|b_{\mp\frac{1}{2}}\rangle|T_{\pm1}\rangle\,, \tag{2.5}$$

$$|\Sigma^*_{b,\pm\frac{1}{2}}\rangle = \sqrt{\frac{2}{3}}\,|b_{\pm\frac{1}{2}}\rangle|T_0\rangle + \sqrt{\frac{1}{3}}\,|b_{\mp\frac{1}{2}}\rangle|T_{\pm1}\rangle\,, \qquad |\Sigma^*_{b,\pm\frac{3}{2}}\rangle = |b_{\pm\frac{1}{2}}\rangle|T_{\pm1}\rangle\,. \tag{2.6}$$

The relative probabilities to produce S_0 and $T_{0,\pm1}$ around the b quark control the relative size of direct Λ_b production and its production from decays of various $\Sigma_b^{(*)}$ states. These probabilities can be parameterized in terms of two nonperturbative parameters, $0 < A < \infty$ and $0 \le w_1 \le 1$ [11],

$$P[S_0] = \frac{1}{1+A}\,, \qquad P[T_0] = \frac{A}{1+A}(1-w_1)\,, \qquad P[T_{+1}] = P[T_{-1}] = \frac{A}{1+A}\frac{w_1}{2}\,. \tag{2.7}$$

$P[T_{-1}]$ and $P[T_{+1}]$ are equal because QCD is parity invariant. The parameters A and w_1 are inclusive over the momentum fraction z of the Λ_b inside the b jet. They do, however, have a weak dependence on the hard scale, Q, as discussed in appendix C. In the remainder of this section we discuss what is known about the values of A and w_1.

The parameter A is the ratio of the $\Sigma_b^{(*)}$ production rate and the direct Λ_b production rate. While the CDF collaboration has measured the masses and widths of the $\Sigma_b^{(*)}$ [32, 33], it has not determined their production rates. We therefore estimate A using the *statistical hadronization model* (for a brief overview, see ref. [34]), according to which the production

JHEP11(2015)067

rate per degree of freedom is proportional to

$$e^{-m/T}\,, \tag{2.8}$$

where m is the mass of the hadron and $T \simeq 165\,\text{MeV}$ [34]. This gives

$$A \simeq 2.6\,, \tag{2.9}$$

for both the bottom and the charm systems.

The value in eq. (2.9) is significantly larger than the estimate in ref. [11], which set $A = 9\,\text{PARJ}(4)$, where PARJ(4) is the `Pythia6` parameter in the Lund fragmentation model describing the probability for forming a spin-1 vs. spin-0 diquark [35, 36], and the factor of 9 is the multiplicity ratio of isotriplet spin-1 and isosinglet spin-0 diquark states. The equivalent `Pythia8` parameter is StringFlav:probQQ1toQQ0 [37]. Depending on the choice of the `Pythia` tune [36, 37] this gives values of A between 0.24 and 0.45. The discrepancy with the estimate in the statistical model is likely due to the fact that the `Pythia` tunes are based on light hadrons. There is no reason to expect this phenomenological parameter to have the same value for heavy-quark hadrons. On the other hand, the quark-diquark model of heavy-baryon production in ref. [38] predicts $A \simeq 6$ for both the bottom and the charm systems. Though somewhat larger, this is of the same order of magnitude as our generic estimate in eq. (2.9). The measurement of the relative Σ_c/Λ_c yield by E791 [39] gives a somewhat smaller value than eq. (2.9), $A \simeq 1.1$ (in extrapolating to Σ_c^* we included the factor R from eq. (3.31), discussed below). The measurement of Σ_b and Σ_b^* production by DELPHI [40], in combination with eq. (2.2), gives $1 \lesssim A \lesssim 10$, again favoring eq. (2.9) over the `Pythia` parameter.

The parameter w_1 accounts for the possibility that the fragmentation axis breaks the rotational symmetry in the spin-1 diquark production. The isotropic case is when $w_1 = 2/3$. DELPHI studied the angular distribution of $\Sigma_b^* \to \Lambda_b\pi$ decays at LEP [40–42] finding

$$w_1 = -0.36 \pm 0.30 \pm 0.30\,. \tag{2.10}$$

Since negative values of w_1 are not physically meaningful this suggests that $w_1 \simeq 0$. In contrast, an analogous measurement in the charm system by CLEO at CESR gave [43]

$$w_1 = 0.71 \pm 0.13\,, \tag{2.11}$$

consistent with the isotropic case. A theoretical calculation [38] based on a quark-diquark model gives $w_1 \simeq 0.41$ and $w_1 \simeq 0.39$ for the bottom and charm system, respectively. The uncertainties on these estimates due to assumptions made in ref. [38] may be large. For instance, finite-width effects, describing the interference between Σ_b and Σ_b^*, are quite important (cf. section 3.2.2), but were neglected in ref. [38]. For these reasons, we shall treat w_1 as a yet-unknown parameter. For other discussions of w_1, and an analogous parameter $w_{3/2}$ relevant to excited mesons, see refs. [11, 44–49].

JHEP11(2015)067

Parameter	(MeV)
$m_{\Sigma_b} - m_{\Lambda_b}$	194 ± 2
$m_{\Sigma_b^*} - m_{\Lambda_b}$	214 ± 2
$\Delta \equiv m_{\Sigma_b^*} - m_{\Sigma_b}$	21 ± 2
Γ_{Σ_b}	7 ± 3
$\Gamma_{\Sigma_b^*}$	9 ± 2

Parameter	(MeV)
$m_{\Sigma_c} - m_{\Lambda_c}$	167.4 ± 0.1
$m_{\Sigma_c^*} - m_{\Lambda_c}$	231.9 ± 0.4
$\Delta \equiv m_{\Sigma_c^*} - m_{\Sigma_c}$	64.5 ± 0.5
Γ_{Σ_c}	2.2 ± 0.2
$\Gamma_{\Sigma_c^*}$	15 ± 1

Table 1. Measured charge-averaged masses and widths of $\Sigma_b^{(*)}$ (left) and $\Sigma_c^{(*)}$ (right) [51]. Σ_c is also known as $\Sigma_c(2455)$, and Σ_c^* as $\Sigma_c(2520)$.

3 Λ_b polarization and $\Sigma_b^{(*)}$ decays

When the b quark emerges from the hard process, it loses only about $2\alpha_s/3\pi \sim 3\%$ of its polarization to gluon radiation [50]. During the fragmentation process, in the exact heavy-quark limit, $m_b/\Lambda_{\rm QCD} \to \infty$, the QCD interactions cannot change the spin of the b quark because its chromomagnetic moment is proportional to $1/m_b$. This is the case for all b hadrons. The additional special property of the Λ_b is that in the heavy-quark limit its light degrees of freedom form a spin-0 state, and thus do not affect the spin of the b throughout the Λ_b lifetime.

As pointed out in ref. [11], the dominant depolarization effect is that the final Λ_b sample contains contributions from b's hadronizing into $\Sigma_b^{(*)}$ that subsequently decay to Λ_b. In the $\Sigma_b^{(*)}$, depolarizing chromomagnetic interaction between the spins of the b quark and the diquark acts over relatively long timescales given by the $\Sigma_b^{(*)}$ lifetimes. We have $\Gamma_{\Sigma_b^{(*)}} < \Delta \ll \Lambda_{\rm QCD}$, where

$$\Delta \equiv m_{\Sigma_b^*} - m_{\Sigma_b} \tag{3.1}$$

is the hyperfine splitting, see table 1 (left). Therefore, hadronization to distinct mass eigenstates $\Sigma_b^{(*)}$ occurs before they decay. Since some of the $\Sigma_b^{(*)}$ states are not eigenstates of the b-quark spin, see eqs. (2.5)–(2.6), the depolarization effect can be of $\mathcal{O}(1)$.

This effect vanishes in the $m_b \to \infty$ limit. In this limit, the decay widths $\Gamma_{\Sigma_b^{(*)}}$, given by the HQET expression in eq. (3.19) below, remain largely unchanged because $m_{\Sigma_b^{(*)}} - m_{\Lambda_b}$ is approximately independent of m_b. The hyperfine mass splitting, on the other hand, scales as $\Delta \propto 1/m_b$, so that for large enough m_b one has $\Gamma_{\Sigma_b^{(*)}} \gg \Delta$ and no depolarization occurs. However, this is not the situation realized in nature.

In the rest of this section we describe the $\Sigma_b^{(*)}$ production and decays and how these influence the Λ_b polarization. We show that the polarization of Λ_b's from $\Sigma_b^{(*)}$ decays depends on both the magnitude and the direction of the original b-quark polarization. The results will be expressed in terms of the angle θ_p, defined in the $\Sigma_b^{(*)}$ rest frame as the angle between the initial b-quark polarization and the fragmentation axis, which lies along the direction of motion of the b quark (see figure 1). For b quarks from top or Z decays, the electroweak interaction produces longitudinal polarization, namely $\theta_p = 0$. This was

JHEP11(2015)067

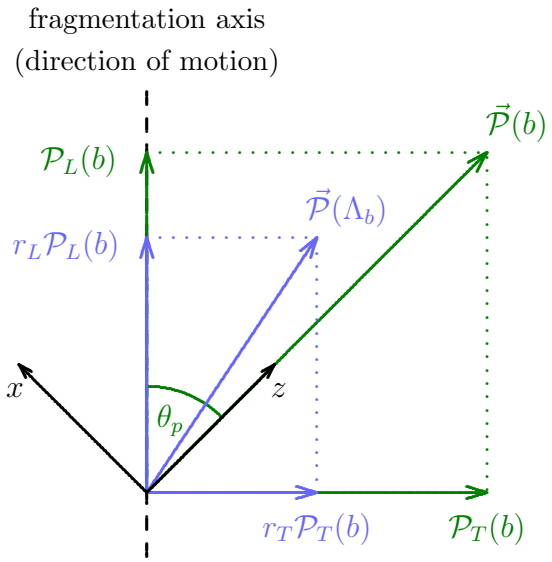

Figure 1. The angle θ_p and the polarization retention factors r_L and r_T.

the only case analyzed in ref. [11]. For b quarks from QCD production, where a small polarization arises at NLO [16], $\theta_p = \pi/2$. In new-physics models, θ_p can in principle have any value. For instance, b quarks produced in decays of a right-handed sbottom to a bino will have a longitudinal polarization of $+1$. Transversely polarized b's can arise, for example, due to a broad resonance interfering with QCD processes, similar to what has been discussed in the context of the transverse polarization of top quarks in ref. [52].

The Λ_c–$\Sigma_c^{(*)}$ system is described by qualitatively the same physics as the Λ_b–$\Sigma_b^{(*)}$ system. The parameters of the relevant baryons are shown in table 1 (right) and the corresponding results for the polarization will be presented in section 3.4.

3.1 Production of $\Sigma_b^{(*)}$ and their decays

We orient our coordinate system such that the b polarization axis in the $\Sigma_b^{(*)}$ rest frame is pointing along the z axis. The parameterization of production probabilities in eq. (2.7) applies to the spin states of the spin-1 diquark along the fragmentation axis, $|T'_{m'}\rangle$. These are expressed in terms of the states along the b polarization axis, $|T_m\rangle$, as

$$\left|T'_{m'}(\theta_p)\right\rangle = \sum_m R_{m'm}(\theta_p)\,|T_m\rangle\ , \tag{3.2}$$

where

$$R_{m'm}(\theta_p) = \begin{pmatrix} \cos^2\frac{\theta_p}{2} & -\frac{\sin\theta_p}{\sqrt{2}} & \sin^2\frac{\theta_p}{2} \\ \frac{\sin\theta_p}{\sqrt{2}} & \cos\theta_p & -\frac{\sin\theta_p}{\sqrt{2}} \\ \sin^2\frac{\theta_p}{2} & \frac{\sin\theta_p}{\sqrt{2}} & \cos^2\frac{\theta_p}{2} \end{pmatrix}\ , \tag{3.3}$$

JHEP11(2015)067

for $m, m' = -1, 0, +1$. Combining a b-quark state with spin $+\frac{1}{2}$ along the z axis with a diquark spin state $|T'_{m'}\rangle$ we obtain

$$|b_{+\frac{1}{2}}\rangle|T'_{m'}(\theta_p)\rangle = \sum_m R_{m'm}(\theta_p)\left[\sum_M \langle\frac{1}{2}, M \,|\, \frac{1}{2}, +\frac{1}{2};\, 1, m\rangle\, |\Sigma_b(M)\rangle + \sum_M \langle\frac{3}{2}, M \,|\, \frac{1}{2}, +\frac{1}{2};\, 1, m\rangle\, |\Sigma_b^*(M)\rangle\right], \quad (3.4)$$

where M is the spin component of the $\Sigma_b^{(*)}$ along the z axis.

In the heavy b-quark limit, the decays $\Sigma_b^{(*)} \to \Lambda_b \pi$ proceed via the decay of the internal spin-1 diquark, $T_{0,\pm1}$, to the spin-0 diquark, S_0, leaving the b quark and its spin unaffected. Since the initial diquark has spin 1, while the final diquark and the pion are spinless, the orbital angular momentum state of the decay products must be $\ell = 1$. Therefore, a $\Sigma_b^{(*)}$ spin state described by J, M decays to a state of the form

$$|\Psi(J, M)\rangle \propto \int d\cos\theta\, d\phi \sum_s \langle\frac{1}{2}, s;\, 1, M - s \,|\, J, M\rangle\, Y_1^{M-s}(\theta, \phi)\, |\theta, \phi\rangle\, |s\rangle\,. \quad (3.5)$$

Here, θ, ϕ describe the direction of motion of the pion in the $\Sigma_b^{(*)}$ frame, s is the Λ_b spin along the z axis, and $Y_\ell^m(\theta, \phi)$ are the spherical harmonics.

3.2 Effect of $\Sigma_b^{(*)}$ decays on Λ_b polarization

3.2.1 Λ_b polarization in the limit of narrow $\Sigma_b^{(*)}$

For simplicity, we first assume that the $\Sigma_b^{(*)}$ widths, $\Gamma_{\Sigma_b^{(*)}}$, can be neglected relative to the mass splitting $\Delta = m_{\Sigma_b^*} - m_{\Sigma_b}$. In this case Σ_b^* and Σ_b decay incoherently since the different pion energies in their final states prevent interference. Taking into account the amplitudes for producing the various $\Sigma_b^{(*)}$ spin states based on eq. (3.4) and the decay amplitudes from eq. (3.5), an initial state $|b_{+\frac{1}{2}}\rangle|T'_{m'}(\theta_p)\rangle$ produces the state

$$|\Psi\rangle \propto \int d\cos\theta\, d\phi \sum_m R_{m'm}(\theta_p) \sum_M \langle J, M \,|\, \frac{1}{2}, +\frac{1}{2};\, 1, m\rangle \times \times \sum_s \langle\frac{1}{2}, s;\, 1, M - s \,|\, J, M\rangle\, Y_1^{M-s}(\theta, \phi)\, |\theta, \phi\rangle\, |s\rangle\,, \quad (3.6)$$

with $J = \frac{1}{2}$ and $\frac{3}{2}$ for the Σ_b's and Σ_b^*'s, respectively. We shall assume that the pion degrees of freedom $|\theta, \phi\rangle$ will not be used in the measurement due to experimental difficulties discussed in section 6. By tracing over the pion degrees of freedom we readily obtain the density matrix of the Λ_b spin

$$\rho_\Psi \propto \mathrm{Tr}_{\theta,\phi}\, |\Psi\rangle\, \langle\Psi|\,, \quad (3.7)$$

where $\Psi = \Sigma_b$ or Σ_b^*.

The total density matrix, combining both Σ_b and Σ_b^* decays, is given by

$$\rho \propto \sum_\Psi p_\Psi \rho_\Psi\,, \quad (3.8)$$

JHEP11(2015)067

where p_Ψ is the probability to produce a particle of type Ψ. From eq. (3.4), $p_{\Sigma_b^*}/p_{\Sigma_b} = 2$. This factor receives a small correction from the fact that a heavier state is less likely to be produced in fragmentation — the Boltzmann factor in eq. (2.8) suppresses Σ_b^* production relative to Σ_b production by a factor of

$$R \equiv e^{-\Delta/T} \simeq 0.88\,. \tag{3.9}$$

The deviation of R from unity is an $\mathcal{O}(\Lambda_{\rm QCD}/m_b)$ effect and we have been neglecting other effects that are formally of the same order. However, keeping $R \neq 1$ will facilitate comparison with the results of the next section, where we go beyond the narrow-width approximation. Furthermore, measurements in the D–D^* system, which is analogous to the Σ_b–Σ_b^* system [11], point to the phenomenological relevance of $R \neq 1$. As discussed in ref. [53] and references therein, the well-measured deviation of the D/D^* multiplicities ratio from the naïve prediction is in agreement with the expectation from the statistical hadronization model. At the same time, the spin alignment of D^* mesons is in agreement with expectations from Clebsch-Gordan coefficients without requiring $1/m_c$ corrections [54]. Combining the production probabilities from eq. (3.4) with this additional correction factor, we rewrite the total density matrix as

$$\rho \propto \rho_{\Sigma_b} + 2R\,\rho_{\Sigma_b^*}\,. \tag{3.10}$$

As a last step we average the contributions to ρ from all diquark spin components m' with relative probabilities determined by the parameter w_1 from eq. (2.7).

Finally, we normalize the density matrix to $\mathrm{Tr}\,\rho = 1$ and use the relation

$$\rho = \frac{1}{2}\left(1 + \vec{\mathcal{P}}\cdot\vec{\sigma}\right) \tag{3.11}$$

to determine the polarization $\vec{\mathcal{P}}$. By symmetry, the polarization in our case can only lie in the xz plane, the plane formed by the initial b polarization and the fragmentation axis. Eq. (3.11) is thus explicitly

$$\rho = \frac{1}{2}\left[(1+\mathcal{P}_z)\,|{\uparrow}\rangle\langle{\uparrow}| + (1-\mathcal{P}_z)\,|{\downarrow}\rangle\langle{\downarrow}| + \mathcal{P}_x\left(|{\uparrow}\rangle\langle{\downarrow}| + |{\downarrow}\rangle\langle{\uparrow}|\right)\right]. \tag{3.12}$$

The two components of the polarization vector are

$$\mathcal{P}_z = \frac{2R - 1 + 2\,(1+R)\,w_1 + (1+R)\,(2-3w_1)\sin^2\theta_p}{3\,(1+2R)}\,, \tag{3.13}$$

$$\mathcal{P}_x = \frac{1+R}{1+2R}\left(w_1 - \frac{2}{3}\right)\sin\theta_p\cos\theta_p\,. \tag{3.14}$$

Above we included only Λ_b's produced from $\Sigma_b^{(*)}$ decays, while directly produced Λ_b's will be added below.

For generic θ_p the polarization vector changes direction relative to the polarization of the original b. This means that $r_{\hat{\mathcal{P}}}$ in eq. (1.1) is a tensor in general. However, if the initial b-quark polarization axis and the fragmentation axis are collinear, $\theta_p = 0$ or π, or

JHEP11(2015)067

are orthogonal to each other, $\theta_p = \pi/2$, the polarization direction remains unchanged, as expected by symmetry. A longitudinally polarized b quark therefore results in a longitudinally polarized Λ_b and a transversely polarized b quark in a transversely polarized Λ_b. For isotropic diquark production, $w_1 = 2/3$, the magnitude of the final polarization is independent of θ_p and its direction is unchanged, as expected.

For a longitudinally polarized b quark, $\theta_p = 0$, the general result in eq. (3.13) reduces to

$$\mathcal{P}_z^L = \frac{2R - 1 + 2\,(1+R)\,w_1}{3\,(1+2R)} \simeq 0.09 + 0.45 w_1\,, \tag{3.15}$$

and for a transversely polarized b quark, $\theta_p = \pi/2$, to

$$\mathcal{P}_z^T = \frac{4R + 1 - (1+R)\,w_1}{3\,(1+2R)} \simeq 0.55 - 0.23 w_1\,. \tag{3.16}$$

Including the direct Λ_b production from fragmentation, the corresponding polarization retention factors from eq. (1.1) are

$$r_{L,T} = \frac{1 + A\,\mathcal{P}_z^{L,T}}{1+A}\,. \tag{3.17}$$

3.2.2 Λ_b polarization for finite $\Sigma_b^{(*)}$ widths

The $\Sigma_b^{(*)}$ widths are only two to three times smaller than their mass splitting, cf. table 1. Sizeable interference effects may thus be present, so we extend our calculation to the case of finite widths. After the production of a Σ_b–Σ_b^* superposition state with energy E, and its decay to $\Lambda_b\pi$, the state vector is

$$\begin{aligned} |E\rangle \propto \int d\cos\theta\, d\phi \sum_m R_{m'm}(\theta_p) \sum_{J,M} \langle J, M \,|\, \frac{1}{2}, +\frac{1}{2};\, 1, m\rangle \, \frac{p_\pi(E)}{E - m_J + i\Gamma(E)/2} \times \\ \times \sum_s \langle \frac{1}{2}, s;\, 1, M-s \,|\, J, M\rangle\, Y_1^{M-s}(\theta,\phi)\, |\theta,\phi\rangle\, |s\rangle\,. \end{aligned} \tag{3.18}$$

Here m_J is the mass of Σ_b or Σ_b^* for $J = \frac{1}{2}, \frac{3}{2}$, respectively. The pion-momentum factor $p_\pi(E) \simeq \sqrt{(E - m_{\Lambda_b})^2 - m_\pi^2}$ derives from the pion coupling in heavy-baryon chiral perturbation theory [22, 55]. Correspondingly, for the width function $\Gamma(E)$ in the propagator we use

$$\Gamma(E) = \frac{g_A^2}{6\pi f_\pi^2}\, p_\pi^3(E)\,, \tag{3.19}$$

where $f_\pi \simeq 93\,\text{MeV}$. This should satisfy $\Gamma(m_{\Sigma_b^{(*)}}) \simeq \Gamma_{\Sigma_b^{(*)}}$. We take the axial-vector current coupling g_A to be 0.63 instead of 0.75 measured in neutron decay, to better reproduce the measured $\Sigma_b^{(*)}$ and $\Sigma_c^{(*)}$ decay widths (see table 1). This choice corresponds to $\Gamma_{\Sigma_b} \simeq 6.1\,\text{MeV}$, $\Gamma_{\Sigma_b^*} \simeq 10.7\,\text{MeV}$, $\Gamma_{\Sigma_c} \simeq 2.1\,\text{MeV}$, and $\Gamma_{\Sigma_c^*} \simeq 15.7\,\text{MeV}$.

We then proceed as in the previous section. From the density matrix

$$\rho(E) \propto \text{Tr}_{\theta,\phi}\, |E\rangle\, \langle E| \tag{3.20}$$

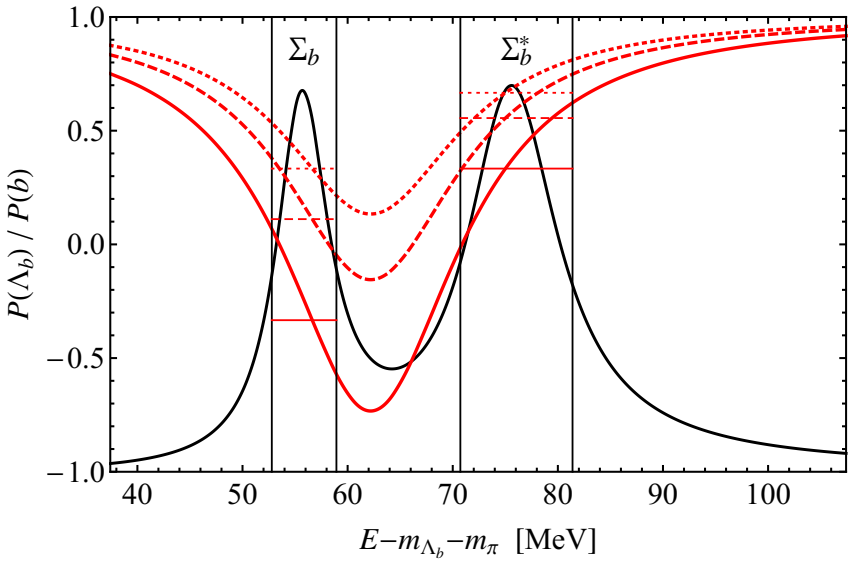

Figure 2. Polarization of Λ_b's produced from $\Sigma_b^{(*)}$ decays as a function of the $\Sigma_b^{(*)}$ energy E. The polarization (red curves) is shown for the longitudinal case with $w_1 = 0$ (solid), 2/3 (dashed) and 1 (dotted). The Σ_b and Σ_b^* production peaks are shown in black (arbitrary y scale). Vertical lines show $\pm\Gamma_{\Sigma_b^{(*)}}/2$ ranges around the nominal masses, and horizontal lines indicate the values of the polarization in the narrow-width limit.

we find the polarization of Λ_b's produced from $\Sigma_b^{(*)}$'s with energy E to be

$$\mathcal{P}_z^L(E) = 1 - 2(2 - w_1)f(E)\,, \qquad \mathcal{P}_z^T(E) = 1 - (2 + w_1)f(E)\,, \tag{3.21}$$

in the longitudinal and transverse case, respectively, where

$$f(E) = \frac{4\,(m_{\Sigma_b^*} - m_{\Sigma_b})^2}{12\,[2(E - m_{\Sigma_b})^2 + (E - m_{\Sigma_b^*})^2] + 9\,\Gamma^2(E)}\,. \tag{3.22}$$

The resulting behavior is shown in figure 2 for the case of longitudinal polarization.

Since we assume that the pion is not identified we average the polarization over E. The corresponding density matrix is

$$\rho \propto \int_{m_{\Lambda_b}+m_\pi}^{\infty} dE\, p_\pi(E)\, e^{-E/T} \rho(E)\,, \tag{3.23}$$

where the $p_\pi(E)$ factor accounts for phase-space integration; this is in addition to two such factors already present in $\rho(E)$ via eq. (3.18). The Boltzmann factor with $T \simeq 165\,\text{MeV}$ is the equivalent of eq. (2.8).

Numerically, we find the polarizations of Λ_b's from $\Sigma_b^{(*)}$ decays in the longitudinal and transverse scenarios to be

$$\mathcal{P}_z^L \simeq 0.23 + 0.38 w_1\,, \qquad \mathcal{P}_z^T \simeq 0.62 - 0.19 w_1\,. \tag{3.24}$$

These results should be compared with eqs. (3.15) and (3.16) that were derived in the narrow-width approximation. We see that finite-width effects are non-negligible.

JHEP11(2015)067

The overall polarization retention factors from eq. (1.1), as computed from eq. (3.24) using eqs. (3.17) and (2.9), are

$$r_L \simeq 0.45\,,\, 0.63\,,\, 0.72\,, \qquad r_T \simeq 0.72\,,\, 0.63\,,\, 0.58\,, \tag{3.25}$$

for $w_1 = 0,\, 2/3,\, 1$, respectively. If we allow the parameter A to differ from our estimate in eq. (2.9) by up to a factor of two, the ranges of possible values of r_L and r_T extend to $0.36 \lesssim r_L \lesssim 0.78$ and $0.52 \lesssim r_T \lesssim 0.78$. The polarization for arbitrary θ_p is given by

$$P_z = r_L \cos^2\theta_p + r_T \sin^2\theta_p\,, \qquad P_x = (r_L - r_T)\sin\theta_p \cos\theta_p\,. \tag{3.26}$$

In appendix A, we derive approximate analytic expressions that describe the results we obtained here. We also present an alternative picture of the physics, in which the depolarization happens due to oscillations between b-spin eigenstates, analogous to K^0–$\overline{K}^0$ oscillations.

3.3 Results from LEP

The Λ_b polarization has been measured, although with a large uncertainty, in Z decays at LEP, using the semileptonic decays of the Λ_b. The polarization of b's produced in Z decays is expected to be longitudinal and given by

$$\mathcal{P}(b) = \frac{-2v_b a_b}{v_b^2 + a_b^2} \simeq -0.94\,, \tag{3.27}$$

where $v_b = -1 + \frac{4}{3}\sin^2\theta_w$ and $a_b = -1$ are factors in the vector and axial-vector couplings of the Z to b quarks. QCD corrections reduce this value by about 3% [50].

ALEPH and DELPHI used the variable $\langle E_\ell\rangle/\langle E_\nu\rangle$ proposed in ref. [56] (for a review of earlier literature on the subject, see ref. [57]), obtaining

$$\mathcal{P}(\Lambda_b) = -0.23\,^{+0.24}_{-0.20}\,(\text{stat.})\,^{+0.08}_{-0.07}\,(\text{syst.}) \qquad (\text{ALEPH [12]}), \tag{3.28}$$

$$\mathcal{P}(\Lambda_b) = -0.49\,^{+0.32}_{-0.30}\,(\text{stat.}) \pm 0.17\,(\text{syst.}) \qquad (\text{DELPHI [14]}), \tag{3.29}$$

while OPAL used a fit to the E_ℓ/E_ν distribution, obtaining

$$\mathcal{P}(\Lambda_b) = -0.56\,^{+0.20}_{-0.13}\,(\text{stat.}) \pm 0.09\,(\text{syst.}) \qquad (\text{OPAL [13]}). \tag{3.30}$$

Even though the precise value of the polarization retention factor r_L cannot be determined from these results due to the large uncertainties, they do suggest that some polarization loss is present (i.e., $r_L = 1$ is excluded), but still r_L is $\mathcal{O}(1)$. Both facts are in agreement with expectations, see eq. (3.25). Large values of w_1 seem to be disfavored, especially by the ALEPH result.

3.4 The charm case

The ideas of this section can also be applied to c quarks. Similarly to eq. (3.9) we have

$$R_{\Lambda_c} \simeq 0.68\,, \tag{3.31}$$

JHEP11(2015)067

with which we find the Λ_c polarizations from $\Sigma_c^{(*)}$ decays in the longitudinal and transverse scenarios to be

$$\left(\mathcal{P}_z^L\right)_{\Lambda_c} \simeq 0.07 + 0.46 w_1\,, \qquad \left(\mathcal{P}_z^T\right)_{\Lambda_c} \simeq 0.54 - 0.23 w_1\,, \tag{3.32}$$

to be compared with eq. (3.24) for the Λ_b. The total polarization retention factors for $w_1 = 0,\, 2/3,\, 1$ are

$$\left(r_L\right)_{\Lambda_c} \simeq 0.33\,,\, 0.55\,,\, 0.66\,, \qquad \left(r_T\right)_{\Lambda_c} \simeq 0.66\,,\, 0.55\,,\, 0.50\,, \tag{3.33}$$

respectively. If we allow the parameter A to differ from our estimate in eq. (2.9) by up to a factor of 2, the ranges of possible values extend to $0.22 \lesssim \left(r_L\right)_{\Lambda_c} \lesssim 0.73$ and $0.42 \lesssim \left(r_T\right)_{\Lambda_c} \lesssim 0.74$.

An important caveat is that $\mathcal{O}(\Lambda_{\rm QCD}/m_c)$ corrections are likely to be larger than the $\mathcal{O}(\Lambda_{\rm QCD}/m_b)$ corrections that we have been neglecting in the b system. In particular, it may no longer be a good approximation to neglect the polarization loss in the initial stage of the fragmentation occurring at the QCD timescale. Nevertheless, even with these effects, the polarization retention factors are likely to remain $\mathcal{O}(1)$. This is supported by the observation that even the Λ's produced in $Z \to jj$ decays at LEP retain an $\mathcal{O}(1)$ fraction of the strange-quark polarization [58–60]. It should be noted that much of the polarization reduction in the case of Λ's at LEP is not due to polarization loss during the s-quark hadronization, but because of an $\mathcal{O}(1)$ contamination from unpolarized Λ's produced from s quarks appearing in the fragmentation process [60]. Such contaminations are expected to be smaller in the Λ_c case. A large transverse Λ_c polarization was measured in QCD processes in the fixed-target experiments NA32 [20] and E791 [21], but theoretical interpretation of these results is difficult (see also ref. [61]) because the typical p_T's of the Λ_c's ($\sim 1.5\,\text{GeV}$) were not much larger than the QCD scale.

4 b-quark polarization measurement via semileptonic Λ_b decays

Here and in the next section we outline several possible strategies for Λ_b and Λ_c polarization measurements in ATLAS and CMS. The ultimate goal is to study b- and c-quark polarizations in new-physics processes. As a SM calibration we propose the $t\bar{t}$ sample. The top decay acts as a "standard candle", fixing the polarization retention factor r_L of b quarks (from primary top decay) and of c quarks (from W decay). In both cases, the polarization of the initial quark is to a good approximation completely left-handed, i.e., $\mathcal{P}(b) \simeq -1$, $\mathcal{P}(c) \simeq -1$ in our convention.

4.1 Properties of the decay

To measure the Λ_b polarization one can use its *inclusive* semileptonic decay

$$\Lambda_b \to X_c\, \ell^- \bar{\nu}\,, \tag{4.1}$$

proceeding via the partonic $b \to c\, W^{-*} \to c\, \ell^- \bar{\nu}$ transition. Here, X_c is an inclusive final state with nonzero charm quantum number. The branching ratio is $\mathcal{B}(\Lambda_b \to X_c\, \ell^- \bar{\nu}) \sim 10\%$

JHEP11(2015)067

for each lepton flavor [51]. The kinematic distributions of the charged lepton and neutrino in eq. (4.1) have been obtained using operator product expansion and HQET, and are under good theoretical control [62]. They are

$$\frac{1}{\Gamma_{\Lambda_b}}\frac{d\,\Gamma_{\Lambda_b}}{d\cos\theta_i} = \frac{1}{2}\left(1+\alpha_i\,\mathcal{P}\left(\Lambda_b\right)\cos\theta_i\right), \qquad i=\ell \text{ or } \nu\,, \tag{4.2}$$

where θ_ℓ (θ_ν) is the angle in the Λ_b rest frame between the lepton (neutrino) momentum and the Λ_b polarization. The distribution is uniform in the azimuthal angle ϕ_ℓ (ϕ_ν). At leading order in $\Lambda_{\rm QCD}/m_b$ and α_s, the coefficients $\alpha_{\ell,\nu}$ multiplying the Λ_b polarization, sometimes called the *spin-analyzing powers* or the *decay asymmetry parameters*, are

$$\alpha_\ell = \frac{-\frac{1}{3}+4x_c+12x_c^2-\frac{44}{3}x_c^3-x_c^4+12x_c^2\log x_c+8x_c^3\log x_c}{1-8x_c+8x_c^3-x_c^4-12x_c^2\log x_c} \simeq -0.26\,, \tag{4.3}$$

$$\alpha_\nu = 1\,, \tag{4.4}$$

where $x_c = m_c^2/m_b^2$. There are no corrections to eqs. (4.3) and (4.4) at $\mathcal{O}(\Lambda_{\rm QCD}/m_b)$, while $\mathcal{O}(\Lambda_{\rm QCD}^2/m_b^2)$ corrections [62] are negligible for our purposes. Higher-order corrections in α_s are also small; they increase α_ℓ by $\sim 5\%$ and decrease α_ν by $\sim 1\%$ [63, 64].

For longitudinally polarized b quarks, the angles θ_ℓ and θ_ν should be measured with respect to the Λ_b flight direction. This is the case for b quarks from Z and top decays and in many new-physics models. For b quarks from QCD production, the polarization is perpendicular to the plane formed by the b quark and colliding partons [16].

$\overline{\Lambda}_b$'s of opposite polarization give the same distributions as eq. (4.2). This means that in Z or $t\bar{t}$ events, for example, the decay products are distributed in the same way relative to the b-jet axis regardless of whether the jet originates from an initial b or $\bar{b}$ quark.

We note that the neutrino is more sensitive to the Λ_b polarization than the charged lepton, see eqs. (4.3), (4.4). The polarization measurement requires knowing the Λ_b rest frame and thus it is necessary to reconstruct the neutrino momentum regardless of whether it is used as a spin analyzer. Another benefit of using the neutrino is that inclusively α_ν is very close to maximal. Therefore, it must remain close to 1 also if we restrict the analysis to a not-too-small subset of the semileptonic decays. This is advantageous since different semileptonic decay modes or kinematic regions may have different efficiencies, either due to experimental limitations or due to cuts applied for background reduction. An important intrinsic background arises from semileptonic B-meson decays. Even though these decays are isotropic, their presence in the sample dilutes the observables sensitive to the Λ_b polarization.

4.2 Strategy for Λ_b-polarization measurement

We suggest to measure the forward-backward asymmetry of the neutrino, $\mathcal{A}_{FB}$, in the Λ_b rest frame along the expected direction of polarization,

$$\mathcal{A}_{FB} = \frac{N_+ - N_-}{N_+ + N_-}\,. \tag{4.5}$$

JHEP11(2015)067

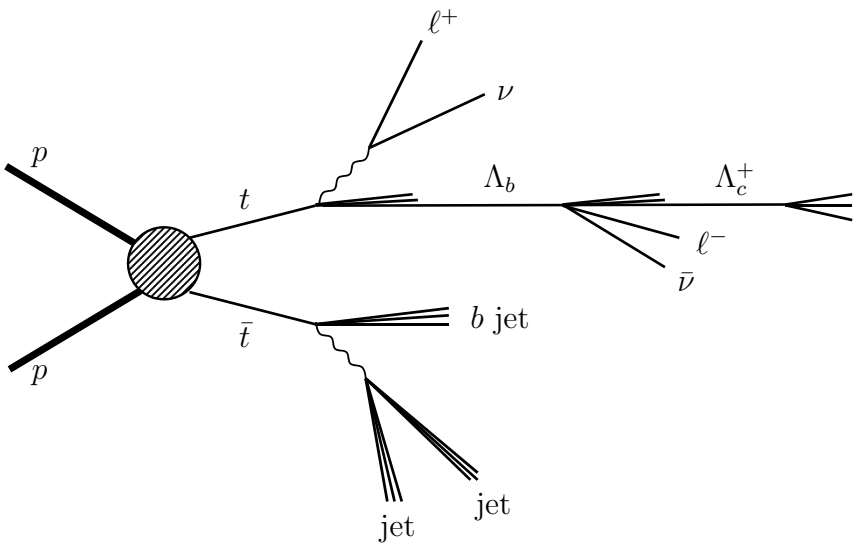

Figure 3. An example $t\bar{t}$ event that can be used for measuring the polarization of b quarks produced in top decays.

Here, N_+ and N_- are the numbers of events with $\cos\theta_\nu > 0$ and $\cos\theta_\nu < 0$, respectively. The neutrinos in signal events are distributed according to eq. (4.2) while in the semileptonic decays of B mesons they are distributed isotropically. As long as the B-meson decays are reconstructed correctly they simply dilute the asymmetry. $\mathcal{A}_{FB}$ then measures the polarization as

$$\mathcal{P}(\Lambda_b) = \frac{2\mathcal{A}_{FB}}{f\,\alpha_\nu}\,, \tag{4.6}$$

where f is the signal event fraction. The statistical uncertainty on $\mathcal{A}_{FB}$ is

$$\Delta\mathcal{A}_{FB} = \sqrt{\frac{1-\mathcal{A}_{FB}^2}{N}}\,, \tag{4.7}$$

where $N = N_+ + N_-$ is the total number of events.

In the rest of this subsection we propose how to tag b jets with $\Lambda_b \to X_c\ell\bar{\nu}$, reconstruct the X_c, and reconstruct the neutrino. Here, we keep the discussion general, but in subsection 4.3 we will analyze, as an explicit example, the polarization measurement of b quarks produced in top decays, illustrated in figure 3. We will estimate the sensitivity of the proposed strategy using efficiencies of similar procedures available in the experimental literature.

We focus on measurements of $\mathcal{P}(\Lambda_b)$ inclusive over the Λ_b momentum fraction, z. This is sufficient as an initial calibration and is the only type of measurement that needs to be performed on new-physics samples. The next experimental step would be measuring $\mathcal{P}(\Lambda_b)$ in SM calibration samples in bins of z, which will provide inputs to the RG running of the polarization retention factors as explained in the introduction and appendix C.

4.2.1 "Soft muon" b tagging

Most LHC analyses apply standard b-tagging algorithms based on the lifetimes of the b-flavored hadrons and/or the b-quark mass. A better choice for our purposes is a "soft muon"

JHEP11(2015)067

b-tagging algorithm. It demands a muon among the jet constituents, where the muon need not be isolated (unlike the hard lepton from the $t \to W \to \ell$ chain in section 4.3 below). The muon impact parameter and its transverse momentum with respect to the jet axis, $p_T^{\rm rel}$, give additional discrimination from non-b-flavored jets.

The reason why "soft lepton" b tagging is not a popular choice in high-p_T analyses is that its efficiency is limited by the sum of the $b \to \ell$ and $b \to c \to \ell$ branching ratios (roughly 10% each [51], times two lepton flavors). For the Λ_b-polarization measurement we already want to use just the semileptonic decays, so this alternative b tagging is actually a high-efficiency option. We focus on $b \to \mu$ rather than on $b \to e$ decays because of the cleaner identification of muons in a typical hadron-collider detector.

We estimate the performance of the "soft muon" b tagging using the CMS public note [65]. Ref. [65] gives the efficiency of selecting b jets versus the rejection rate for non-b jets, separately for selections based on $p_T^{\rm rel}$ and for the impact parameter. Requesting a large impact parameter is somewhat more effective than requesting large $p_T^{\rm rel}$ against light-flavored jets. However, this is largely due to the contribution from the $b \to c \to \mu$ decay chain, which in our case is not part of the signal. As an example working point we therefore choose a $p_T^{\rm rel}$-based selection that gives a survival probability of $\epsilon_{udsg} \simeq 0.3\%$ for jets initiated by u, d, s quarks or by gluons, $\epsilon_c \simeq 2.5\%$ for jets initiated by c quarks, and $\epsilon_b = 8\%$ for true b-flavored jets. The value for ϵ_b is inclusive, encompassing b quarks decaying directly into a muon, $b \to \mu$, decaying indirectly, $b \to c \to \mu$, or with no muon at all in the decay chain. For jets whose initial b-quark decay chain does contain a prompt muon ($b \to c\mu\nu$) the tagging efficiency is approximately 70%.

4.2.2 X_c reconstruction

The inclusive X_c state in $\Lambda_b \to X_c\mu\nu$ usually contains a Λ_c baryon, which often decays into a Λ. We examine three Λ_b selections in order of decreasing statistics, but increasing purity,

- *Inclusive selection:* requiring only the presence of a soft muon inside a jet,
- *Semi-inclusive selection:* requiring in addition the presence of a $\Lambda \to p\pi^-$ candidate,
- *Exclusive selection:* completely reconstructing a Λ_c candidate in a few clean modes with only charged particles in the final state.

The studies of Λ_b in QCD events [17–19, 28] use $\Lambda_b \to J/\psi\,(\to \mu^+\mu^-)\,\Lambda\,(\to p\pi^-)$. Using this decay would provide a cleaner sample than the three approaches described above, but it has a very small branching ratio of $\sim 3.2 \times 10^{-5}$. This requires large statistics, making it prohibitive to use in new-physics processes. Another clean decay used by LHCb [66], $\Lambda_b \to J/\psi\,(\to \mu^+\mu^-)\,pK^-$, likely also suffers from a small branching ratio (not yet reported). However, these decays can become useful in the future for cross-checking and refining the information obtained from SM calibration samples like $t\bar{t}$ using the semileptonic decays on which we focus here.

To measure the Λ_b polarization it is necessary to reconstruct the neutrino and Λ_b momenta. This is equivalent to knowing the $X_c\mu$ and neutrino momenta. In this subsection

JHEP11(2015)067

we explain how the $X_c\mu$ momentum is determined in each of the above selections. In the next subsection we use this information to also obtain the neutrino momentum.

Inclusive selection. In this approach we only require the soft muon, which for the signal events originates from Λ_b decays. (There is also a small contribution from polarized Ξ_b baryons, discussed in appendix B.) An important background is semileptonic B decays. Even though these decays are isotropic, their presence in the sample dilutes the observables sensitive to the Λ_b polarization, cf. eq. (4.6). In the inclusive selection the purity of the sample is small, $\mathcal{O}(f_{\rm baryon})$, as the branching ratios of semileptonic Λ_b and B decays are very similar. On the positive side, the data set is very large. As an estimate for $\mathcal{B}(\Lambda_b \to X_c\mu\nu)$ in our numerical estimates we shall use $\mathcal{B}(\Lambda_b \to \Lambda_c\mu\nu + \text{anything}) \simeq 10\%$ [51], neglecting the small contribution from decays in which X_c contains a D meson rather than the Λ_c baryon (see discussion below).

In this inclusive approach the Λ_b four-momentum can be determined only approximately, and on a statistical basis. For b quarks produced at energies near the electroweak scale, the Λ_b carries on average only $\langle z\rangle \sim 70\%$ of the b-quark energy, with a broad distribution [67–70]. Approximating the z distribution with its average, we write

$$E_{\Lambda_b} \simeq \langle z\rangle E_b\,. \tag{4.8}$$

To estimate the $X_c\mu$ energy, we first correct the measured jet energy, $E_{\rm jet}$, by subtracting the energies of charged tracks originating from the primary vertex (assuming they are $\pi^\pm$) to obtain $E'_{\rm jet}$. To get the $X_c\mu$ energy one would need to also subtract the energy of neutral particles from the primary vertex (mostly due to π^0's), $E_{\rm neutral}$,

$$E_{X_c\mu} = E'_{\rm jet} - E_{\rm neutral}\,. \tag{4.9}$$

However, $E_{\rm neutral}$ cannot be experimentally distinguished from neutral particles from the Λ_b decay. We thus make an approximation; the probability for a pion to be a π^0 is $\sim 1/3$, so on average

$$E_{\rm neutral} \simeq \frac{1-\langle z\rangle}{3}\,E_b\,. \tag{4.10}$$

Using eq. (4.8) and $E_{\Lambda_b} = E_{X_c\mu} + E_\nu$ we express $E_{X_c\mu}$ in terms of the corrected jet energy and the yet-unknown neutrino energy as

$$E_{X_c\mu} \simeq \frac{3\langle z\rangle E'_{\rm jet} - (1-\langle z\rangle)E_\nu}{2\langle z\rangle + 1} \simeq \frac{3\langle z\rangle}{2\langle z\rangle + 1}\,E'_{\rm jet}\,. \tag{4.11}$$

In the last step we neglected the E_ν term since it is typically an order of magnitude smaller than the first term. The same procedure works for the background decays $B \to X_c\mu\nu$.

We also need to determine the momentum, $\vec{P}_{X_c\mu}$. While the muon is readily identifiable and measurable, the momentum of X_c requires additional approximations. In cases where X_c contains just a (ground-state or excited) charmed hadron, the direction of $\vec{P}_{X_c}$ can be taken as the direction of the track-based jet it produces and its magnitude can be determined from E_{X_c} assuming $m_{X_c} \simeq m_{\Lambda_c}$. It is not crucial to use the precise c-hadron mass since the parent b-hadron mass is relatively large. If X_c contains additional charged

JHEP11(2015)067

hadrons, typically pions, observed as tracks originating from the b-hadron decay vertex, their momenta can be included trivially, and their energies subtracted from E_{X_c} (assuming they are $\pi^{\pm}$) to obtain the charmed-hadron energy. More problematic are neutral hadrons, which contribute energy to the jet but do not leave tracks. One cannot determine whether they come directly from the b-hadron decay (in which case they need to be treated separately) or only from the subsequent c-hadron decay (in which case they are included in $m_{X_c} \simeq m_{\Lambda_c}$). The former case is problematic. It is not very common since usually X_c is a single charmed hadron — $\mathcal{B}(\Lambda_b \to \Lambda_c \mu\nu) \sim 0.7\,\mathcal{B}(\Lambda_b \to \Lambda_c \mu\nu + \text{anything})$, $\mathcal{B}(B^0 \to D^{(*)}\mu\nu) \sim 0.8\,\mathcal{B}(B^0 \to D^{(*)}\mu\nu + \text{anything})$, $\mathcal{B}(B^{\pm} \to D^{(*)}\mu\nu) \sim 0.8\,\mathcal{B}(B^{\pm} \to D^{(*)}\mu\nu + \text{anything})$ [51], and only a fraction of the remaining decays are expected to contain π^0's. However, despite the small size of these contributions, misreconstruction of such events in the background can potentially contribute a large bias to the measured $\mathcal{A}_{FB}$, considering the low signal-to-background ratio of this inclusive selection.

One possible handle for reducing the background from $B \to D$ decays is the shortness of the Λ_c lifetime relative to the D-meson lifetimes: $\tau_{D^{\pm}}/\tau_{\Lambda_c} \simeq 5$, $\tau_{D_s^{\pm}}/\tau_{\Lambda_c} \simeq 2.5$, $\tau_{D^0}/\tau_{\Lambda_c} \simeq 2$. This is even more significant than the difference between D- and B-meson lifetimes, which is already being used by ATLAS as one of the handles for tagging c jets while rejecting b jets [71, 72]. For example, the *loose* operating point from ref. [71] provides 95% efficiency for c jets with a factor of 2.5 rejection of b jets. Perhaps an analogous technique could be used in our case for accepting Λ_c's while rejecting a significant fraction of D mesons. While designing the relevant algorithms or estimating their expected performance is beyond the scope of this paper, we encourage further work along this direction and note that the shortness of the Λ_c lifetime has already been used for background reduction in a Λ_b study by D0 [73].

It may also be possible to estimate the background contribution and subtract it. One could, for instance, use high-p_T b jets from QCD events as a control sample. In this case the b's have no longitudinal polarization, so that the measured $\mathcal{A}_{FB}$ will be entirely due to misreconstruction. One could further improve the accuracy of the background prediction using *embedding*: for the process of interest one would first select a sample of fully reconstructed b-decay events, and then replace the b jet with a kinematically equivalent semileptonic b jet from the QCD sample (with the momentum determined from the rest of the QCD event). Here we do not pursue these ideas further but rather consider less inclusive selections that significantly suppress the background contributions, while keeping the overall statistical uncertainties comparable to that of the inclusive selection.

Semi-inclusive selection. The large background from semileptonic B decays can be reduced by requiring among the jet constituents both a soft muon and a Λ baryon. In the vast majority of $\Lambda_b \to X_c \ell\nu$ decays we expect the X_c to contain a Λ_c.[2] We can then use the decay chain $\Lambda_c \to \Lambda(\to p\pi^-) + X$, with $\mathcal{B}(\Lambda_c \to \Lambda + X) \simeq 0.35$ and $\mathcal{B}(\Lambda \to p\pi^-) \simeq 0.64$. Requiring a reconstructed $\Lambda \to p\pi^-$ decay inside the b jet and originating from the vicinity

[2]Experimentally, for example, $\mathcal{B}(\Lambda_b \to D^0 p\pi^-) \sim 0.1 \times \mathcal{B}(\Lambda_b \to \Lambda_c^+ \pi^-)$ [51]. We expect $\Lambda_b \to D^0 p\ell^-\bar{\nu}$ to be suppressed relative to $\Lambda_b \to \Lambda_c \ell^-\bar{\nu}$ by a similar factor and thus $\Lambda_b \to X_c \ell\nu$ to be dominated by $\Lambda_b \to \Lambda_c \ell\nu + X$ decays.

JHEP11(2015)067

Decay mode	Branching fraction
$\Lambda_c^+ \to p\,K^-\pi^+$	6.7%
$\Lambda_c^+ \to \Lambda\pi^+ \to p\,\pi^+\pi^-$	0.9%
$\Lambda_c^+ \to p\,K_S \to p\,\pi^+\pi^-$	1.1%
$\Lambda_c^+ \to \Lambda\pi^+\pi^+\pi^- \to p\,\pi^+\pi^+\pi^-\pi^-$	2.2%
$\Lambda_c^+ \to p\,K_S\pi^+\pi^- \to p\,\pi^+\pi^+\pi^-\pi^-$	1.2%

Table 2. Branching fractions of the main all-charged decays of Λ_c. For $\Lambda_c^+ \to p\,K^-\pi^+$, we used the average from ref. [26] dominated by the recent Belle measurement [76] instead of the much less precise PDG value of $(5.0 \pm 1.3)\%$ [51]. The ratio of the two values was used to rescale the other branching fractions from their PDG values, since they were measured relative to $\Lambda_c^+ \to p\,K^-\pi^+$.

of the displaced vertex will eliminate most of the B-meson background. Some B-meson contamination may still be present due to $K_S^0 \to \pi^+\pi^-$ decays mimicking $\Lambda \to p\pi^-$. This can be suppressed with a modest efficiency loss by requiring that the invariant mass of the two tracks, if assumed to be pions, is incompatible with the known K_S^0 mass [28].

A reconstructed Λ in the jet can also be used for reducing the background from $\Lambda_b \to \Lambda_c + X$ with the Λ_c decaying semileptonically. While in principle the sign of the lepton eliminates this background, this requires knowing whether the jet originated from a b or a $\bar{b}$. Sometimes this information is available from the rest of the event, e.g., in a reconstructed $t\bar{t}$ sample from the sign of the lepton in a leptonically decaying top [74]. If not, one can use the relative signs of the lepton and the Λ decay products.

In the numerical estimates we will assume an $\epsilon_\Lambda \simeq 30\%$ efficiency for $\Lambda \to p\pi^-$ reconstruction. This is larger than the efficiency of 10–16% quoted by CMS in ref. [28] because we believe that quality cuts can be relaxed. The maximal achievable efficiency is limited by tracking efficiency, which is around 60%, considering the pair of tracks in $\Lambda \to p\pi^-$ and integrating over the $c\tau$ distribution of the Λ [75]. It should be noted though that the installation of new tracking detectors in ATLAS and CMS in the next years will likely significantly improve the reconstruction efficiency of long-lived resonances like the Λ baryon.

In the semi-inclusive selection, X_c reconstruction is approximate, performed using the same procedure as for the inclusive selection.

Exclusive selection. In this approach the hadronic system X_c is reconstructed very precisely by first reconstructing Λ_c from its decay products in one of the channels where all the products are charged, and then adding charged particles whose vertices are compatible with the reconstructed Λ_c origin. The strongest point of this approach is that one can obtain the Λ_c four-momentum without approximations. X_c is then known completely if the Λ_c is accompanied only by charged particles, and is known approximately if there are neutral particles like π^0. Moreover, purity against B mesons is expected to be high. All this comes at a moderate cost in statistics. Table 2 summarizes the most promising Λ_c decay modes. The dominant one has $\mathcal{B}(\Lambda_c^+ \to p\,K^-\pi^+) \simeq 6.7\%$ [26]. CDF have already

JHEP11(2015)067

used this channel for studying the Λ_b [27]. Second in size are the modes with an additional vertex from Λ or K^0_S decays, which have a total branching ratio of around 5.4% [26, 51]. D0 have already used one of these channels ($\Lambda_c^+ \to pK_S \to p\,\pi^+\pi^-$) for studying the Λ_b [73]. It may be noted that restricting the analysis to just a fraction of the Λ_c decays does not invalidate the inclusiveness assumption in eq. (4.1) on which eq. (4.4) relies, as long as all $\Lambda_b \to \Lambda_c + X$ decays are included.

The reconstruction efficiencies achievable for the decays in table 2, which involve between three and five charged particles in the final state and in part of the cases an intermediate resonance, should be estimated with a detailed detector simulation. We note that CMS has reported 33% efficiency for the three-prong decay $B^+ \to J/\psi(\to \mu^+\mu^-)K^+$ for $p_T^{B^+} > 30\,\text{GeV}$ [77] and 20% efficiency for the four-prong decay $B_s^0 \to J/\psi(\to \mu^+\mu^-)\,\phi(\to K^+K^-)$ for $23 < p_T^{B_s^0} < 50\,\text{GeV}$ [78] in inclusive QCD production. For $D^+ \to K^-\pi^+\pi^+$ decays in $W + c$ production, CMS had about 11% efficiency for $p_T^{c-\text{jet}} > 25\,\text{GeV}$ [79] and ATLAS had 32% efficiency for $p_T^{D^+} > 8\,\text{GeV}$ [80]. In the following, we therefore assume that on average an efficiency of $\epsilon_{\Lambda_c} \simeq 25\%$ is achievable for the Λ_c reconstruction.

4.2.3 "Soft neutrino" reconstruction

Knowing the $X_c\mu$ four-momentum together with the flight direction of Λ_b suffices to determine the soft-neutrino momentum up to a two-fold ambiguity [81] (see also ref. [82]). Experimentally, the Λ_b flight direction is the direction between the primary vertex and the secondary vertex associated with the soft muon. The neutrino momentum perpendicular (parallel) to the Λ_b flight direction, $P_\nu^\perp$ ($P_\nu^\parallel$), is

$$P_\nu^\perp = -P_\perp\,, \qquad P_\nu^\parallel = -a \pm \sqrt{b}\,, \tag{4.12}$$

where

$$a = \frac{(m_{\Lambda_b}^2 - m^2 - 2P_\perp^2)P_\parallel}{2(P_\parallel^2 - E^2)}\,, \qquad b = \frac{(m_{\Lambda_b}^2 - m^2 - 2P_\perp^2)^2E^2}{4(P_\parallel^2 - E^2)^2} + \frac{E^2P_\perp^2}{P_\parallel^2 - E^2}\,. \tag{4.13}$$

Here, $P_\perp$, $P_\parallel$, E and m are the $X_c\mu$ system's momenta perpendicular and parallel to the Λ_b flight direction, its energy, and its invariant mass, respectively. Eq. (4.12) gives two real solutions for $P_\nu^\parallel$ if $b > 0$, and two complex solutions if $b < 0$. We propose to discard events with complex solutions since the backgrounds are more likely to have negative b values. The two real solutions can be treated on equal footing, as in refs. [81, 82], as both carry information on the neutrino momentum although with different resolution. However, we illustrate in section 4.3.2 how for the $t\bar{t}$ example the full-event information can be used to solve the ambiguity.

The precision of the neutrino reconstruction is limited by the uncertainty on the direction between the primary and the secondary vertex. The angular uncertainty is

$$\delta\alpha \simeq \frac{\delta x}{\gamma_{\Lambda_b}\, c\tau_{\Lambda_b}}\,, \tag{4.14}$$

where δx is the uncertainty on the relative position of the two vertices and γ_{Λ_b} is the boost factor. It should be compared with the typical angle α of the neutrino momentum, which

JHEP11(2015)067

for $\gamma_{\Lambda_b} \gg 1$ is, very roughly,

$$\alpha \simeq \frac{P_\nu^\perp}{P_\nu} = \frac{\left(P_\nu^\perp\right)_{\text{rest}}}{P_\nu} \sim \frac{m_{\Lambda_b}/5}{P_{\Lambda_b}/3} \simeq \frac{0.6}{\gamma_{\Lambda_b}}\,. \tag{4.15}$$

This gives

$$\frac{\delta\alpha}{\alpha} \sim 0.2 \left(\frac{\delta x}{50\ \mu\text{m}}\right) \left(\frac{\tau_{\Lambda_b}}{1.45 \times 10^{-12}\ \text{s}}\right)^{-1}, \tag{4.16}$$

independent of γ_{Λ_b}. Even though this uncertainty is non-negligible, it is not prohibitive.

The method outlined here is applicable to any sample of b quarks. In cases where the rest of the event does not contain invisible particles, e.g., $pp \to Z \to b\bar{b}$, $pp \to b\bar{b}$ with the second b in the event identified as decaying hadronically, one can also use the measured $\vec{\not{E}}_T$ as input to reconstruction.

4.3 Measurement in $pp \to t\bar{t}$ events

We now apply the general strategy for measuring the Λ_b polarization to $pp \to t\bar{t}$ events. We estimate its sensitivity, under several simplifying assumptions, for 100 fb^{-1} at 13 TeV LHC. Performing such an analysis in ATLAS or CMS would be very useful for calibrating the b-quark polarization measurement. Given the approximate universality of the polarization retention factor r_L, see introduction and appendix C, the value extracted from the $t\bar{t}$ sample would be an important input when measuring the polarization of b quarks produced in new-physics processes.

The analysis strategy that we propose consists of the following steps: selection of a $t\bar{t}$-enriched sample by requiring an isolated lepton and at least four high-p_T jets; reconstruction of a Λ_b candidate; global event interpretation in terms of jet-parton assignment and reconstruction of the neutrinos by the exploitation of kinematic constraints; measurement of the forward-backward asymmetry of the soft neutrino in an opportunely chosen rest frame.

4.3.1 Event selection

The best compromise between statistics and selection purity is achieved by targeting the final state with a single isolated electron or muon from W-boson decay, for which the total branching ratio is approximately 30%. Final states with two isolated leptons give better selection purity but the branching ratio is six times smaller; an all-hadronic selection could achieve a reasonable selection purity only by imposing very tight kinematic thresholds. An additional benefit of the single-isolated-lepton sample is that one can veto the decay chain $b \to cX \to \ell\nu X'$ using the relative sign of the isolated lepton from the W boson and the non-isolated lepton from the Λ_b (see section 4.2.1), in conjunction with global event interpretation (section 4.3.2).

As an example, we take as baseline the same selection as in ref. [83], a $t\bar{t}$ analysis in the single-leptonic final state based on about 20 fb^{-1} of 8 TeV data, in which traditional b tagging is not applied. This analysis requires exactly one isolated lepton with $p_T > 26$ GeV and $|\eta| < 2.1(2.4)$ in the muon (electron) channel, and at least four hadronic jets with

JHEP11(2015)067

$p_T > 30\,\text{GeV}$ and $|\eta| < 2.4$. In this way, $208(230) \times 10^3$ events in the muon (electron) channel are selected, out of which $86(100) \times 10^3$ are estimated from detailed simulation to be genuine $t\bar{t}$ events. Most of the background is composed of W+jets events, with smaller contributions from multi-jet QCD production, Drell-Yan, and single-top processes.

Going from 8 TeV to 13 TeV collisions, the $t\bar{t}$ cross section increases by a factor 3.3 [84]. If we assume similar selection efficiencies as for 8 TeV we expect 1.4 (1.65) million $t\bar{t}$ events in the muon (electron) channel for 100 fb^{-1} of integrated luminosity. The cross section for the main background, the inclusive W-boson production, increases by 1.9 (as calculated at NNLO with `FEWZ 3.1` [85, 86]), but there are large uncertainties on the fraction of events with four associated jets above the p_T threshold.

After the soft-muon selection of section 4.2.1 is applied to the events passing the baseline selection, we expect roughly 540 000 $t\bar{t}$ and 17 000 single-top events (mostly tW) [87] to remain in the Run 2 dataset. Here, the yields for isolated-muon and isolated-electron channels have been summed. The rejection of non-top backgrounds depends on the poorly measured fraction of heavy-flavored jets associated with W, Z and $\gamma^\star$ production. Taking the associated jet multiplicity and heavy-flavor compositions of these samples predicted by `MadGraph` [88] with standard settings, and assuming that the multi-jet QCD background can be neglected, we expect less than 30 000 background events.

The above estimates can be viewed as conservative. One can increase statistics by adding a "soft electron" b tagging. Moreover, the global event interpretation, outlined in the next subsection, can be used to further increase the signal-to-background ratio by selecting mass windows around the nominal masses of the reconstructed top-quark and W-boson candidates. In the rest of the section we therefore simplify the discussion and ignore all non-top and single-top processes, focusing completely on the true $t\bar{t}$ events. The expected numbers of events are summarized in table 3, in which we also list the expected numbers of events after the three approaches to $X_c\mu$ reconstruction.

4.3.2 Global event interpretation

The $\Lambda_b \to X_c\mu\nu$ reconstruction procedure described in section 4.2.3 determines the soft-neutrino momentum, and correspondingly the Λ_b momentum, up to a two-fold ambiguity. This ambiguity can be resolved by checking which of the two hypotheses is more consistent with the kinematics of the full $t\bar{t}$ event, since the reconstructed b-quark momentum and the missing energy that would be attributed to the hard neutrino from $t \to Wb \to \ell\nu b$, differ between the two solutions.

The global event interpretation is also useful for vetoing events in which the soft muon and the soft neutrino come from a $b \to c \to \mu\nu$ cascade. Such events can be rejected by requiring that this muon has the same (opposite) sign as the hard lepton coming from the opposite (same) reconstructed top quark in the event. This is important mostly in the inclusive approach to X_c reconstruction from section 4.2.2, where the charges of the X_c constituents are not measured.

There exist various approaches to kinematic reconstruction of events with tops (e.g. refs. [89–95]). An important issue is that standard algorithms misreconstruct the $t\bar{t}$ event in a large fraction of the cases. For example, a radiation jet sometimes provides a better

JHEP11(2015)067

Selection	Expected events		
Baseline	3×10^6 $t\bar{t}+\mathcal{O}(10^6)$ bkg		
Soft-muon b tagging	5×10^5 $t\bar{t}+\mathcal{O}(10^4)$ bkg		
Signal events ($t\to b\to\Lambda_b\to\mu\nu X_c$)		Purity (example)	$\Delta\mathcal{A}_{FB}/\mathcal{A}_{FB}$
Inclusive	34 400	$\mathcal{O}(f_{\text{baryon}})$ (e.g., 7%)	±7%
Semi-inclusive	$2300\times(\epsilon_\Lambda/30\%)$	70%	±8%
Exclusive	$1040\times(\epsilon_{\Lambda_c}/25\%)$	30%	±19%
		100%	±10%

Table 3. Approximate number of expected $t\bar{t}$ events surviving different selections in the Λ_b polarization analysis, for 100 fb^{-1} at 13 TeV. Baseline selection indicates the request of exactly one isolated lepton (electron or muon) and at least four jets, as in ref. [83]. ϵ_Λ is the efficiency of $\Lambda\to p\pi^-$ reconstruction, ϵ_{Λ_c} the efficiency of Λ_c reconstruction in the channels of table 2. Events originating from both b and $\bar{b}$ are included in all numbers. In the last column, the expected statistical uncertainty on the soft-neutrino asymmetry for the different selections described in section 4.2.2 is reported assuming the indicative purity in the third column and $r_L=0.6$.

fit to one of the nominal $t\bar{t}$ products than the actual corresponding jet, especially when the latter is mismeasured or falls outside of acceptance. While extensive simulation would be necessary to determine which algorithms are best in our context and what their performance is, we would like to make several remarks.

First, the reconstruction does not need to be fully correct for our purposes. In particular, a correct reconstruction of just the top quark that produced the Λ_b suffices for resolving the soft-neutrino ambiguity and for vetoing events with wrong-sign leptons. It may even be beneficial in some cases to focus on reconstructing the relevant top rather than insist on reconstructing both. Also, even when the event is completely misreconstructed, the soft-neutrino solution will still be correct (accidentally) in roughly half of the cases.

Second, we note that in the standard $t\bar{t}$ reconstruction approaches, the possibility that a significant fraction of the b-quark momentum is carried by a neutrino is not taken into account. The prevalence of such events degrades the overall resolution of the reconstruction. Since we account for the soft neutrino explicitly, the reconstruction in our case will profit to some extent from this, usually ignored, additional information. The resulting impact on the performance of event interpretation depends on the applied algorithm and its estimation is beyond the scope of this paper.

In the sensitivity estimates below, we will optimistically neglect the potential impacts of misreconstructed events. However, note that even if the $t\bar{t}$ reconstruction were completely useless (which is an unreasonably pessimistic assumption), one could keep both soft-neutrino solutions and account for this ambiguity when interpreting the results, as was done in refs. [81, 82].

JHEP11(2015)067

4.3.3 Expected sensitivity

After resolving the ambiguity in the soft-neutrino momentum as outlined above, we apply the asymmetry analysis of section 4.2. In the last column of table 3 we collect estimates for the purely statistical component of $\Delta\mathcal{A}_{FB}/\mathcal{A}_{FB}$ that follow from eqs. (4.6) and (4.7), assuming as an example $r_L = 0.6$, cf. eq. (3.25). These will also be the statistical uncertainties on the value of r_L extracted from these measurements.

We see that despite the different degrees of inclusiveness the three selections have comparable statistical uncertainties. Therefore, the fully inclusive selection is disfavored, considering the background reconstruction uncertainties discussed in section 4.2.2. The amount of background in the semi-inclusive approach is much more manageable, although the measurement would still be somewhat limited by the systematics related to the approximations made in the reconstruction of the X_c 4-momentum in the signal. The vertexing uncertainty described in eq. (4.16) is common to all the three approaches. Since many of the systematic uncertainties depend on experimental details that are difficult for us to simulate using publicly available tools, and since the first measurement will likely be limited by statistics, the detailed study of systematic uncertainties is deemed outside the scope of this work.

Overall, this looks like a promising measurement for Run 2 of the LHC.

5 c-quark polarization measurement via $\Lambda_c^+ \to pK^-\pi^+$ decays

In principle, the semileptonic decays of Λ_c are similar to those of Λ_b. In this case it is the charged lepton rather than the neutrino that has approximately maximal spin-analyzing power. Unfortunately, the semileptonic channel seems impractical. First, its branching ratio is small, $\mathcal{B}(\Lambda_c \to X\mu\nu) \simeq 3.1\%$ — this estimate follows from rescaling $\mathcal{B}(D^\pm \to X\mu^\pm\nu)$ by the ratio of $\Lambda_c^\pm$ and $D^\pm$ lifetimes. At the same time, semileptonic D decays, which constitute an intrinsic background, have much larger branching ratios, by factors of about 5 and 2 for $D^\pm$ and D^0, respectively. This is different from the Λ_b case where the semileptonic branching ratios of B mesons and Λ_b are similar. Another difficulty is that, due to the relatively short lifetime, $\tau_{\Lambda_c} \simeq 2.0 \times 10^{-13}$ s [51], there is a prohibitively large uncertainty on the Λ_c flight direction reconstructed as the direction between primary and secondary vertices, cf. eq. (4.16). Also the uncertainty due to additional neutral hadrons produced at the primary vertex is larger since they carry a larger fraction of the c-quark momentum than in the b-quark case. Finally, backgrounds with prompt muons become more significant. The reason is the short Λ_c lifetime and the small m_c; they make selection techniques that use impact parameter and relative muon p_T, respectively, much less effective.

A more promising decay mode is $\Lambda_c^+ \to pK^-\pi^+$. Its branching ratio is relatively large, about 6.7% [26], while the D-meson background can be reduced significantly, without losing much signal, by restricting the invariant mass of the three candidate tracks to lie close to the Λ_c mass. For the angular distributions of each of the decay products we expect the same functional form as in eq. (4.2), but theoretical uncertainties on the hadronic matrix elements preclude precise predictions for the values of α_i for p, K^-, and π^+. These can

JHEP11(2015)067

be measured in the SM calibration sample. It may be noted that they can have different values for the different processes contributing to the $pK^-\pi^+$ final state, which include $p\overline{K}^*(892)^0$, $\Delta(1232)^{++}K^-$, $\Lambda(1520)\pi^+$, and non-resonant production [21]. Results from the NA32 experiment [20] indicate that α_{K^-} is $\mathcal{O}(1)$, as was conjectured in ref. [96], while α_p and α_{π^+} are small.

5.1 Strategy for Λ_c-polarization measurement

A way to tag a c jet for the purpose of the polarization measurement is to demand the presence of a candidate $\Lambda_c^+ \to pK^-\pi^+$ decay and consistency with a global event interpretation. As an example for the latter, we discuss in subsection 5.2 the polarization measurement of c quarks from W decays using a $t\bar{t}$ sample (see figure 4).

The identification of $\Lambda_c^+ \to pK^-\pi^+$ decays in ATLAS and CMS is not trivial because the identities of charged hadrons are typically not determined by the detectors.[3] We, therefore, propose the following strategy. Select three candidate tracks based on lifetime and vertexing criteria, i.e., requiring incompatibility with the hypothesis of tracks originating from the primary vertex and compatibility with the hypothesis of coming from a common secondary vertex. The kaon candidate is the track whose charge is opposite to the other two. In some scenarios, the global event interpretation would tell us whether we expect a Λ_c^+ or a $\overline{\Lambda}_c^-$, and then a requirement on the absolute charges of the tracks can be added to reduce the background. Among the remaining two tracks, the one with the higher momentum (in the lab frame) is taken to be the proton candidate, and the other the pion candidate. This is almost always the correct choice for high-p_T Λ_c's because the proton is much heavier than the pion. In the small fraction of cases where this assignment is incorrect, the reconstructed Λ_c mass will typically fall outside the expected range, so the contamination will be minimal. After this identification procedure, the forward-backward asymmetry $\mathcal{A}_{FB}$ of any of the three decay products (p, K, π) in the Λ_c rest frame can be used for the polarization measurement.

Since both the $\Lambda_c^+ \to pK^-\pi^+$ branching fraction, table 2, and the Λ_c fragmentation fraction, eq. (2.3), are small, the intrinsic background from Λ_c decays to other final states (e.g., $\Lambda_c^+ \to pK^-\pi^+\pi^0$, $\Sigma^+\pi^-\pi^+$, $\pi^+\pi^-\pi^+\Lambda$) and D-meson decays (e.g., $D^+ \to \pi^+K^-\pi^+$, $\pi^+K^-\pi^+\pi^0$; $D^0 \to \pi^+K^-\pi^+\pi^-$; $D_s^+ \to K^+K^-\pi^+$, $K^+K^-\pi^+\pi^0$) is a concern even after demanding the invariant mass of the p, K, π candidates to be consistent with m_{Λ_c}. However, there are several effective handles for reducing many of these backgrounds:

- In the signal decay, the kaon momentum in the lab frame is typically in-between the momenta of the pion and the proton, similarly to the discussion above. Demanding such a hierarchy reduces the background since in most of the background decays that contain three charged particles these particles are not p, K^-, π^+ so the negatively charged track does not necessarily tend to be intermediate in momentum.

[3] Although particle-identification procedures based on specific energy loss or time of flight have been developed in both ATLAS and CMS [97–101], they show sufficient separation between protons and lighter hadrons only up to track momenta of $\mathcal{O}$(GeV) at most. This is too small for the end-products of the decays of top quarks or new heavy resonances.

JHEP11(2015)067

- Decays in which one of the three tracks, or an extra neutral particle, is a long-lived strange hadron, can be eliminated by vetoing on additional further-displaced vertices.

- A veto on a fourth track consistent with the candidate Λ_c vertex can eliminate most of the D^0 backgrounds since the D^0 cannot decay to three charged particles.

- The different lifetimes, $\tau(\Lambda_c^+, D^0, D_s^+, D^+) \simeq (2, 4, 5, 10) \times 10^{-13}$ s, can be used for reducing all D-meson backgrounds.

- Backgrounds from particular decays to three charged particles, such as $D^+ \to \pi^+K^-\pi^+$ and $D_s^+ \to K^+K^-\pi^+$, can be targeted by demanding that if the tracks are assigned the masses of these decay products, the resulting invariant mass should be inconsistent with that of the parent D meson.

- Mild cuts on the p_T's of the tracks and of the Λ_c candidate would be beneficial for reducing the background due to secondary hadrons produced in fragmentation (soft Λ_c's and D mesons, as well as other sources of contaminating tracks).

The combination of the above requirements will likely greatly suppress the backgrounds while reducing the signal by less than an order of magnitude. Yet, it is not clear whether the backgrounds will be negligible in the end. The precise amount of background is scenario-dependent. This is because the displaced-vertex properties, the ordering of the three tracks' momenta in the lab frame for both the signal and the backgrounds, and the reconstructed-mass resolution, all depend on the charmed hadron momentum. The signal efficiency and purity will therefore depend on the kinematics of the process producing the c quarks. Estimating those for any particular process requires a detailed simulation and is beyond the scope of this work. In any case, since the Λ_c mass peak is narrow while the backgrounds are smooth, one can use a sideband for estimating and subtracting the bias that the backgrounds may be contributing to $\mathcal{A}_{FB}$. The background under the peak would still contribute statistical fluctuations.

5.2 Measurement in $pp \to t\bar{t}$ events

We now describe the Λ_c polarization measurement in $pp \to t\bar{t}$ events, in which longitudinally-polarized charm quarks are produced via $t \to W^+b \to c\bar{s}b$, as illustrated in figure 4. We estimate the sensitivity for $100\,\text{fb}^{-1}$ at 13 TeV under various simplifying assumptions. Performing such an analysis in ATLAS or CMS would be very useful for calibrating the c-quark polarization measurement. Such a calibration measurement is even more important than for Λ_b, because of possibly large Λ_{QCD}/m_c corrections to r_L and r_T, and the fact that the spin-analyzing powers of the $\Lambda_c^+ \to pK^-\pi^+$ decay are a priori unknown.

The strategy that we propose here is similar to the Λ_b analysis from the previous section. It consists of selecting a $t\bar{t}$-enriched sample by requiring an isolated lepton and at least four high-p_T jets, reconstructing the event, and measuring the forward-backward asymmetry of the proton, kaon, or pion in the Λ_c rest frame.

JHEP11(2015)067

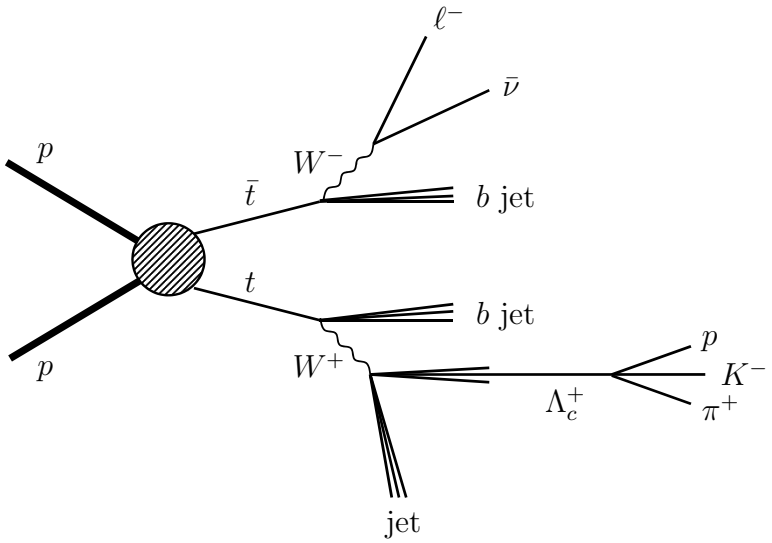

Figure 4. An example $t\bar{t}$ event that can be used for measuring the polarization of c quarks produced in W decays.

We start with a baseline selection of a single lepton and at least four jets similarly to section 4.3.1 and apply standard b-tagging algorithms to remove most non-top background events. As an example we use the efficiencies from ref. [102], where the event selection contains a single isolated lepton (electron or muon) with $p_T > 33\,\text{GeV}$ and $|\eta| < 2.1$, at least four jets with $p_T > 30\,\text{GeV}$ and $|\eta| < 2.4$, and exactly two of the four leading jets are required to pass a b-tagging selection based on the combination of track-based lifetime and secondary vertices information. The b-tagging working point corresponds to $\epsilon_b = 70\%$ [103]. With these selection criteria, 108 205 events survive in $20\,\text{fb}^{-1}$ at 8 TeV with a composition of 94.3% $t\bar{t}$, 3.4% single top (mostly tW), 1.9% W+jets, and 0.4% Z+jets. We, therefore, expect roughly 1.7×10^6 $t\bar{t}$ events for an integrated luminosity of $100\,\text{fb}^{-1}$ at 13 TeV and we can neglect the non-top backgrounds. Event reconstruction can be performed similarly to section 4.3.2. Conventional b-tagging algorithms can be used to assist the assignment of the jets. Λ_c candidates from the two jets interpreted as originating from b quarks should be vetoed. The expected number of signal events after reconstruction, using f_{Λ_c} from eq. (2.3) and $\mathcal{B}(\Lambda_c^+ \to pK^-\pi^+) \simeq 6.7\%$ [26], is shown in table 4.

Let us estimate the expected sensitivity assuming that just one of the Λ_c decay products is being used in the polarization measurement, presumably the one with the largest spin-analyzing power α_i. Since it is likely that α_i is close to 1 for the kaon [20, 96], and the possible values of r_L are given by eq. (3.33), we will present estimates for $\alpha_i r_L = 0.6$. Considering the intrinsic backgrounds discussed in section 5.1, the signal efficiency ϵ_{Λ_c} and purity f cannot be determined without a detailed study. For the purpose of our estimates we assume $\epsilon_{\Lambda_c} = 25\%$ as in section 4.2.2 and consider two possibilities for the purity f: 100% and 20%. The resulting statistical uncertainty on the polarization measurement, $\Delta\mathcal{A}_{FB}/\mathcal{A}_{FB}$, determined along the lines of eqs. (4.6) and (4.7), is shown in the last column of table 4.

Overall, performing this measurement in Run 2 of the LHC seems feasible.

JHEP11(2015)067

Selection	Expected events	Purity (example)	$\Delta\mathcal{A}_{FB}/\mathcal{A}_{FB}$
Baseline	1.7×10^6 $t\bar{t}+\mathcal{O}(10^5)$ bkg		
$\Lambda_c^+ \to pK^-\pi^+$	$810\times(\epsilon_{\Lambda_c}/25\%)$	20%	26%
		100%	11%

Table 4. Approximate number of expected $t\bar{t}$ events surviving different selections in the Λ_c polarization analysis, for 100 fb^{-1} at 13 TeV. Baseline selection indicates the request of exactly one isolated lepton (electron or muon) and two jets passing standard b-tagging selection out of at least four, as in ref. [102]. ϵ_{Λ_c} indicates the efficiency of Λ_c reconstruction in the $\Lambda_c^+ \to pK^-\pi^+$ channel. Events originating from both c and $\bar{c}$ are included in all the numbers. The last column shows the expected statistical uncertainty on the forward-backward asymmetry of the Λ_c decay product with the highest spin-analyzing power α_i, assuming $\alpha_i r_L = 0.6$, for two different assumptions regarding the achievable purity of the selection.

6 Isolating $\Sigma_b^{(*)}$, $\Sigma_c^{(*)}$ decays

As discussed in detail in section 2, a large fraction of Λ_b's are produced from the decays

$$\Sigma_b^{(*)\pm,0} \to \Lambda_b\,\pi^{\pm,0}\,. \tag{6.1}$$

So far, we considered them part of the Λ_b sample. In principle, they can be distinguished from primary Λ_b's by observing a pion that together with the Λ_b reconstructs the $\Sigma_b^{(*)}$ mass. In practical implementations $Q = m(\Lambda_b\pi) - m(\Lambda_b) - m_\pi$ may be a better variable than the $\Sigma_b^{(*)}$ mass, because it reduces resolution effects from the Λ_b reconstruction. Vetoing the $\Sigma_b^{(*)} \to \Lambda_b\,\pi^{\pm,0}$ contributions would eliminate the leading depolarization effect, giving an even more direct correlation between Λ_b and b-quark polarizations. In this section we discuss the prospects for identifying $\Sigma_b^{(*)}$ (and analogously $\Sigma_c^{(*)}$) decays at the LHC.

An immediate difficulty is that the pion is very soft, $m_{\Sigma_b^{(*)}} - m_{\Lambda_b} \sim 0.04 m_{\Lambda_b}$. In the semileptonic channels advocated in section 4 for the b-polarization measurement, the Λ_b reconstruction is not sufficiently precise for reconstructing $\Sigma_b^{(*)}$'s. This is due to the neutrino, whose reconstruction involves non-negligible uncertainties from the direction between the primary and secondary vertex, and due to the ambiguities surrounding neutral particles in the jet. Another difficulty is combinatorial background. The soft pion stems from the primary vertex, where additional pions and other hadrons are frequently produced as part of the jet in the b-quark fragmentation process. In the case of a neutral pion, neutral hadrons produced in the Λ_b decay would contribute an additional ambiguity. It is thus likely that the optimal choice is to treat decayed $\Sigma_b^{(*)}$'s as part of the Λ_b sample, as we have done throughout this paper.

On the other hand, separate studies of $\Sigma_b^{(*)}$ decays in the SM calibration samples, using well-reconstructed Λ_b decay channels where all the final-state particles are charged, could be very useful for better characterization of the polarization-loss mechanisms. The parameter A discussed in section 2 can be determined from the overall yield of these decays. w_1 can be determined either from the angular distribution of the pions (as discussed in ref. [11] and already attempted by DELPHI at LEP [40–42]) or from the Λ_b polarization.

JHEP11(2015)067

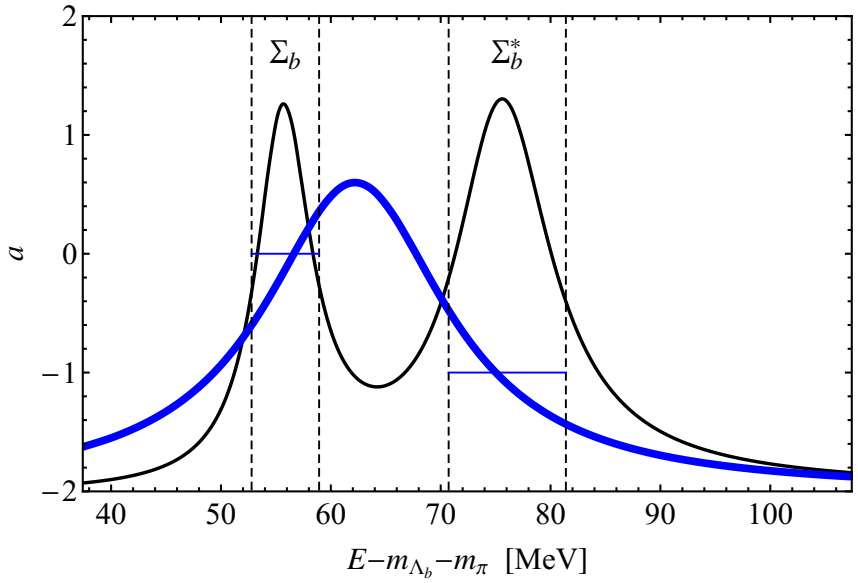

Figure 5. Coefficient a from eq. (6.2) describing the angular dependence in $\Sigma_b^{(*)} \to \Lambda_b\pi$ (thick blue curve) overlaid on top of the $\Sigma_b^{(*)}$ spectrum (black curve, arbitrary y scale). Dashed vertical lines show $\pm\Gamma_{\Sigma_b^{(*)}}/2$ ranges around the nominal masses, and horizontal lines indicate the values of a in the narrow-width limit.

Overconstraining the system would even allow going beyond the dominant polarization-loss effects we consider in this paper.

Using the formalism of section 3.2.2, we find that finite-width effects can be important in determining w_1 from the pion angular distributions. In the $\Sigma_b^{(*)}$ rest frame, relative to the direction of motion of the $\Sigma_b^{(*)}$ in the lab, they are given by

$$\frac{1}{\Gamma}\frac{d\Gamma}{d\cos\theta} = \frac{1}{2} + \frac{9}{8}\,a\left(w_1 - \frac{2}{3}\right)\left(\cos^2\theta - \frac{1}{3}\right) . \tag{6.2}$$

In the narrow-width limit $\Gamma_{\Sigma_b^{(*)}} \ll \Delta$, $a = 0$ for the Σ_b (whose angular distribution is therefore insensitive to w_1) and $a = -1$ for the Σ_b^*. This case was emphasized in ref. [11] and assumed in the DELPHI measurement [40–42]. In the opposite limit, $\Gamma_{\Sigma_b^{(*)}} \gg \Delta$, $a = -2$. More generally, a depends on the reconstructed mass E of the $\Sigma_b^{(*)}$ as

$$a(E) = -2 + \frac{8\,(m_{\Sigma_b^*} - m_{\Sigma_b})^2}{4[2(E - m_{\Sigma_b})^2 + (E - m_{\Sigma_b^*})^2] + 3\Gamma^2(E)} . \tag{6.3}$$

This is plotted in figure 5 for the masses and widths from table 1 and eq. (3.19). The value of a varies significantly within the Σ_b and $\Sigma_b^{(*)}$ peaks, and the average values within each peak may modestly deviate from the narrow-width-limit value, depending on the definition of the peak boundaries. More interestingly, the large widths provide an opportunity for a more precise measurement of w_1. For example, one can focus the analysis on mass ranges with large $|a|$ and/or avoid cancellations of sensitivity between mass ranges with positive and negative values of a as it happens in the Σ_b case.

JHEP11(2015)067

Identifying $\Sigma_b^{(*)}$ decays in ATLAS, CMS, and LHCb seems possible. One relevant Λ_b decay channel is

$$\Lambda_b \to \Lambda_c^+ \pi^- \,, \quad \Lambda_c^+ \to p K^- \pi^+ \,. \tag{6.4}$$

Using this channel, CDF has successfully studied $\Sigma_b^{(*)}$'s at the Tevatron [32, 33], although not the quantities relevant in our context. LHCb has reconstructed Λ_b's in this channel in ref. [30], although without reconstructing $\Sigma_b^{(*)}$'s. In ref. [104] they studied $\Xi_b^{\prime,*} \to \Xi_b \pi$ decays (which are analogous to $\Sigma_b^{(*)} \to \Lambda_b \pi$ decays) using the channel $\Xi_b^0 \to \Xi_c^+ \pi^-$, $\Xi_c^+ \to p K^- \pi^+$. Another possibility is

$$\Lambda_b \to J/\psi \, \Lambda \,, \quad J/\psi \to \mu^+ \mu^- \,, \quad \Lambda \to p \pi^- \,. \tag{6.5}$$

This channel is already being used by ATLAS [18], CMS [19, 28] and LHCb [17] for Λ_b measurements. CMS has also studied $\Xi_b^* \to \Xi_b \pi$ decays using the similar channel $\Xi_b^- \to J/\psi \, \Xi^-$, $J/\psi \to \mu^+ \mu^-$, $\Xi^- \to \Lambda \pi^-$, $\Lambda \to p \pi^-$ [105]. Another possible channel, used by LHCb in ref. [66], is

$$\Lambda_b \to J/\psi \, p \, K^- \,, \quad J/\psi \to \mu^+ \mu^- \,. \tag{6.6}$$

For the decay chain in eq. (6.4), the spin-analyzing power is expected to be close to maximal [25, 106–111]. For the decay chain in eq. (6.5) there is disagreement between different theoretical approaches [25, 107, 110, 112–117], many predicting the analyzing power to be $\mathcal{O}(0.1)$. The analyzing powers of the decay in eq. (6.6) are unknown. Not having a prediction for the spin-analyzing power is not a problem by itself since one can still extract w_1 from the polarization measurement by normalizing the result to a sample not enriched in $\Sigma_b^{(*)}$'s, or from the angular distribution of the pions from $\Sigma_b^{(*)} \to \Lambda_b \pi$ as discussed above.

For the c-quark polarization measurement, the idea of vetoing on $\Sigma_c^{(*)}$ contributions is somewhat more promising. The pion is less soft, $m_{\Sigma_c^{(*)}} - m_{\Lambda_c} \sim 0.09 m_{\Lambda_c}$, and the decay mode advocated in section 5, $\Lambda_c^+ \to p K^- \pi^+$, is fully reconstructible. Reconstruction of $\Sigma_c^{(*)}$'s in this channel has been performed by CDF in ref. [118].

The study of isolated $\Sigma_c^{(*)}$ samples is even more important than $\Sigma_b^{(*)}$ since the information that can be obtained from inclusive Λ_c measurements is possibly limited. In particular, a direct measurement of r_T may be problematic: the polarization in QCD events is sizeable only for momenta $p_c \sim m_c$, which is probably too close to $\Lambda_{\rm QCD}$ for factorization to be reliable. Instead, one may prefer to use the theoretical prediction for r_T (section 3.4), which relies on knowing A and w_1. These two parameters can be obtained from measurements of the $\Sigma_c^{(*)}$ yields and the angular distribution of the pion in $\Sigma_c^* \to \Lambda_c \pi$ decays, respectively. The latter measurement has already been performed by CLEO [43], but it would be desirable to verify its result, eq. (2.11), in view of the apparent discrepancies described at the end of section 2. Direct measurements of A and w_1 would also be useful for comparisons with theoretical models, considering that even in the longitudinal case the polarization measurement is only sensitive to the products $\alpha_i r_L$ and the spin-analyzing powers α_i are unknown. It may be noted that since measurements of A and w_1 do not require a polarized sample, they can also be done in Belle, where high-precision studies of $\Sigma_c^{(*)}$'s have been reported recently [119], and in BaBar.

JHEP11(2015)067

7 Conclusions

We pointed out that b and c-quark polarizations can be measured at the LHC, and designed general techniques that can be used for that purpose in ATLAS and CMS. The most interesting application would be characterization of new-physics processes producing such quarks. While new physics is yet to be discovered, we motivated a set of Standard Model analyses for ATLAS, CMS, LHCb, BaBar, and Belle that would help calibrate the polarization measurements.

Our approach relies on the fact that Λ_b baryons partly preserve the initial b-quark polarization. Since $m_b \gg \Lambda_{\rm QCD}$, the processes that can change the polarization during hadronization are under good theoretical control. The dominant effect is due to $\Sigma_b^{(*)}$ decaying to Λ_b and a pion [11]. While formally suppressed by $1/m_b$, the effect is numerically $\mathcal{O}(1)$ for the values of m_b and $\Sigma_b^{(*)}$ decay widths realized in nature. The depolarization effects can be parametrized by retention factors r_L and r_T for longitudinally and transversely polarized initial b quarks, respectively. Once r_L and r_T are measured in Standard Model calibration samples with known polarization, it will be possible to use them for studying the polarization of b's from possible new-physics processes. The same ideas apply to c quarks and the Λ_c baryons.

Polarization measurements in Standard Model samples will also contribute to our understanding of QCD. As we discussed, there exist several different phenomenological approaches that give somewhat conflicting predictions for the non-perturbative QCD parameters A and w_1 that determine r_L and r_T. Measurements of r_L and r_T in samples of quarks with a known initial polarization would thus be useful for assessing the ranges of validity of the various models. It would also be interesting to compare results obtained for bottom and charm quarks and examine to what extent the differences can be accounted for by higher-order effects in the HQET expansion.

For a Λ_b polarization measurement, the semileptonic decay $b \to c\ell\bar{\nu}$ seems particularly promising, with the neutrino being a perfect spin analyzer. For a Λ_c polarization measurement we suggest using $\Lambda_c^+ \to pK^-\pi^+$.

We proposed to measure r_L for b quarks using $t\bar{t}$ samples in ATLAS and CMS. After single-lepton $t\bar{t}$ baseline selection and identification of a potential Λ_b decay using soft-muon b tagging, the kinematics of the events is reconstructed. The b-quark polarization is then probed by measuring the forward-backward asymmetry of the neutrino in the Λ_b rest frame. We examined several approaches, with varying degrees of purity, for dealing with the intrinsic background due to semileptonic B decays. In all of them, one can measure r_L with about 10% precision using $100\,\text{fb}^{-1}$ of data at the 13 TeV LHC, considering only statistical uncertainties. While a full analysis of systematic uncertainties is beyond the scope of our work, we argued that at least in the high-purity approaches they are not prohibitively large.

For measuring r_L for c quarks, we again proposed to use single-lepton $t\bar{t}$ samples in ATLAS and CMS, where polarized c quarks are produced in W decays. Here, the calibration measurements will determine the products, $r_L\alpha_i$, of the c-quark polarization-retention factor and the spin-analyzing powers for each of the three decay products in $\Lambda_c^+ \to pK^-\pi^+$. With $100\,\text{fb}^{-1}$ of data, a precision of around 10%–30% is attainable.

JHEP11(2015)067

Finally, r_T can be measured in the QCD production of b and c jets. As we discussed, r_L and r_T are different functions of several, currently unknown, QCD parameters. Therefore, measurements of r_L and r_T are complementary. Reconstruction of Λ_b decays from which the polarization can be extracted, in inclusive QCD samples, was performed by LHCb [17], ATLAS [18] and CMS [19]. LHCb reconstructed also Λ_c decays [120]. We note that it will be useful for the polarization measurements in these samples to go beyond the constant-polarization ansatz assumed in [17–19] since the polarization is predicted to be a function of the parton-level kinematics of the event [16].

To reduce theoretical uncertainties it would be helpful to also have analyses that focus on $\Lambda_{b,c}$'s produced from $\Sigma_{b,c}^{(*)}$ decays. Besides studying the polarization of these samples, we argued that it would be useful to measure the $\Sigma_{b,c}^{(*)}$ yields (relative to the inclusive $\Lambda_{b,c}$ yields) and the angular distributions of the pion in $\Sigma_{b,c}^{(*)} \to \Lambda_{b,c}\pi$. These analyses have to be done in fully reconstructible decay modes, where all the final-state particles are charged. Such studies can be performed by ATLAS, CMS, LHCb, and in the charm sector also by BaBar and Belle.

Even though r_L and r_T are mostly universal, i.e., independent of the production mechanism, they do have a weak dependence on the energy scale of the process. Their scale dependence is calculable by relating them to fragmentation functions. The required inputs can be acquired by measuring r_L and r_T at a fixed reconstructed b-quark momentum but binned in the Λ_b momentum (and similarly in the c-quark case) once sufficient data are available.

In short, the initial polarizations of b and c quarks are encoded in the polarizations of Λ_b and Λ_c baryons, respectively. The upcoming Run 2 of the LHC will allow measuring the universal retention factors with $t\bar{t}$ samples.

Acknowledgments

We thank Marco Gersabeck, Gilad Perez, Torbjörn Sjöstrand and Peter Skands for useful correspondence and conversations. The work of YG is supported in part by the U.S. National Science Foundation through grant PHY-0757868 and by the United States-Israel Binational Science Foundation (BSF) under grant No. 2010221. JZ is supported by the U.S. National Science Foundation under CAREER Grant PHY-1151392. The work of AG is partially supported by the Estonian Academy of Science with the Mobilitas Top Researcher Grant MTT59. MG acknowledges the support by the U.S. Department of Energy under grant No. DE-SC0008475.

A More on Λ_b polarization for finite $\Sigma_b^{(*)}$ widths

The results of section 3.2.2 were obtained by evaluating the integral in eq. (3.23) numerically. Here, we derive approximate analytic expressions by taking the energy-dependent factors $p_\pi(E)$ and $e^{-E/T}$ in eqs. (3.18) and (3.23) to be constant factors

$$\sqrt{\Gamma} \quad \text{and} \quad e^{-m/2T} \tag{A.1}$$

JHEP11(2015)067

in eq. (3.18). The energy-dependent widths $\Gamma(E)$ in the propagators are replaced with a constant Γ, and the lower limit of integration in eq. (3.23) is set to $-\infty$.

We still need to specify which constant values to use for the m and Γ. For terms in eq. (3.23) that involve just the Σ_b or just the Σ_b^*, i.e., the non-interfering terms, it makes sense to take m_{Σ_b} and $m_{\Sigma_b^*}$, respectively, for m and similarly Γ_{Σ_b} and $\Gamma_{\Sigma_b^*}$ for Γ (although the dependence on Γ does drop out after the integration in eq. (3.23)). For the interfering terms, on the other hand, it makes more sense to use some effective value $m_{\rm eff}$ between m_{Σ_b} and $m_{\Sigma_b^*}$ and the corresponding $\Gamma_{\rm eff} \equiv \Gamma(m_{\rm eff})$.

We then obtain

$$\mathcal{P}_z = \frac{2R - 1 + 2\,(1+R)\,w_1 + 4R_{\rm eff}\,(2 - w_1)\,/\,\left(x^2+1\right)}{3\,(1+2R)} + \frac{1 + R - 2R_{\rm eff}/\left(x^2+1\right)}{3\,(1+2R)}\,(2 - 3w_1)\sin^2\theta_p\,, \tag{A.2}$$

$$\mathcal{P}_x = \frac{1 + R - 2R_{\rm eff}/\left(x^2+1\right)}{1+2R}\left(w_1 - \frac{2}{3}\right)\sin\theta_p\cos\theta_p\,, \tag{A.3}$$

where R has been defined in eq. (3.9) and similarly $R_{\rm eff} \equiv e^{-(m_{\rm eff} - m_{\Sigma_b})/T}$, and

$$x \equiv \frac{\Delta}{\Gamma_{\rm eff}}\,. \tag{A.4}$$

In the $m_b \to \infty$ limit, Σ_b and Σ_b^* have equal masses and widths, leading to $R = R_{\rm eff} = 1$, $x = 0$, and thus $\mathcal{P}_z = 1$, $\mathcal{P}_x = 0$, as expected. Since in reality x is $\mathcal{O}(1)$, the deviation from the formal $m_b \to \infty$ limit can be large. Even for $R = R_{\rm eff} = 1$ the depolarization can still be $\mathcal{O}(1)$. For instance, taking $w_1 = 2/3$, one has $\mathcal{P}_z = (1 + 11x^2/27)/(1 + x^2)$. In the narrow-width limit, $x \to \infty$, eqs. (A.2)–(A.3) reduce to eqs. (3.13)–(3.14).

Let us now substitute numerical values for $\Gamma_{\rm eff}$ and $R_{\rm eff}$ in eqs. (A.2)–(A.3). For example, values corresponding to $m_{\rm eff} = m_{\Sigma_b}$ give

$$\mathcal{P}_z^L \simeq 0.17 + 0.41 w_1\,, \qquad \mathcal{P}_z^T \simeq 0.59 - 0.21 w_1\,, \tag{A.5}$$

while for $m_{\rm eff} = m_{\Sigma_b^*}$

$$\mathcal{P}_z^L \simeq 0.28 + 0.36 w_1\,, \qquad \mathcal{P}_z^T \simeq 0.64 - 0.18 w_1\,. \tag{A.6}$$

These numbers are close to the exact results in eq. (3.24), which lie between the two cases for $m_{\rm eff}$.

Another point we would like to make is that the physics of spin rotation, which we have been describing in *momentum* space, can also be described as oscillations in *time* between spin eigenstates, similar to K^0–$\overline{K}^0$ oscillations, for example. The b spin in our case is the analog of strangeness, while the Σ_b and Σ_b^* are the analogs of K_L and K_S. With the approximations made in this appendix, it is possible to interpret the physics in this way if we assume a common width Γ for the Σ_b and Σ_b^* and ignore the small effect of the thermal factor. With the Fourier transform

$$\frac{1}{E - m + i\Gamma/2} \propto \int_0^\infty dt\, e^{iEt}\, e^{-imt - \Gamma t/2} \tag{A.7}$$

JHEP11(2015)067

for each of the propagators, we obtain

$$\int_{-\infty}^{\infty} dE\, |E\rangle\, \langle E| \propto \int_{0}^{\infty} dt\; e^{-\Gamma t}\; |\Psi_{m'}(t)\rangle\, \langle \Psi_{m'}(t)| \;, \tag{A.8}$$

where

$$\begin{aligned} |\Psi_{m'}(t)\rangle \propto\; & e^{-im_{\Sigma_b} t} \sum_m R_{m'm}(\theta_p) \sum_M \langle \frac{1}{2}, M \,|\, \frac{1}{2}, +\frac{1}{2};\, 1, m\rangle\, |\Sigma_b(M)\rangle \\ & + e^{-im_{\Sigma_b^*} t} \sum_m R_{m'm}(\theta_p) \sum_M \langle \frac{3}{2}, M \,|\, \frac{1}{2}, +\frac{1}{2};\, 1, m\rangle\, |\Sigma_b^*(M)\rangle \end{aligned} \tag{A.9}$$

describes the time evolution (oscillations) of the state initially given by eq. (3.4). The time-dependent prefactor $e^{-\Gamma t}$ in eq. (A.8) describes the fraction of particles that decay at time t.

B Ξ_b polarization

In the main text we consider the most common hadronization of b into baryons, which is that b hadronizes with u and/or d quarks. However, in roughly 15% of the cases, one of the light quarks is s producing Ξ_b, Ξ_b', Ξ_b^* baryons. These are isospin doublets with spin configurations equal to the ones of Λ_b, Σ_b, Σ_b^*, respectively. The polarization formalism of section 3 thus applies also in this case. Polarized Ξ_b's, produced directly, as well as from Ξ_b' and Ξ_b^* decays, can be used to improve the statistics of the b polarization measurement.

The mass splitting between Ξ_b^* and Ξ_b', $\Delta_{\Xi_b} \simeq 20\,\text{MeV}$, is much larger than their decay widths, $\Gamma_{\Xi_b^*} \simeq 1.6\,\text{MeV}$ and $\Gamma_{\Xi_b'} < 0.08\,\text{MeV}$ [104, 105, 121]. The Ξ_b depolarization due to Ξ_b' and Ξ_b^* decays can therefore be described in the narrow-width limit, eqs. (3.15)–(3.16). The statistical hadronization model gives in this case $A_{\Xi_b} \simeq 1.2$ and $R_{\Xi_b} \simeq 0.91$, consistent with partial information on the relative production rates [104]. The polarizations in the longitudinal and transverse cases are

$$\left(\mathcal{P}_z^L\right)_{\Xi_b} \simeq 0.10 + 0.45 w_1 \,, \qquad \left(\mathcal{P}_z^T\right)_{\Xi_b} \simeq 0.55 - 0.23 w_1 \,, \tag{B.1}$$

giving the total polarization retention fractions (after including direct Ξ_b production)

$$\left(r_L\right)_{\Xi_b} \simeq 0.51\,,\, 0.67\,,\, 0.75\,, \qquad \left(r_T\right)_{\Xi_b} \simeq 0.75\,,\, 0.67\,,\, 0.63\,, \tag{B.2}$$

for $w_1 = 0,\, 2/3,\, 1$, respectively. These values of r_L and r_T are similar to those characterizing Λ_b, eq. (3.25).

If the semileptonic decays of the b are used for the polarization measurement, the possibility discussed in section 4, one might consider performing an inclusive measurement including both Λ_b and Ξ_b contributions. The Ξ_b semileptonic branching ratios are expected to be similar to those of the Λ_b (for one of the dominant decays, $\Xi_b \to \Xi_c \ell\nu$ and $\Lambda_b \to \Lambda_c \ell\nu$, see ref. [122] and references therein). Assuming equal branching ratios, and also that the Ξ_b'–Ξ_b^* system has the same value of w_1 as the Σ_b–Σ_b^* system, the weighted averages that the inclusive measurement would be sensitive to are

$$\left(r_L\right)_{\text{incl.}} \simeq 0.45\,,\, 0.64\,,\, 0.73\,, \qquad \left(r_T\right)_{\text{incl.}} \simeq 0.73\,,\, 0.64\,,\, 0.59\,, \tag{B.3}$$

for $w_1 = 0,\, 2/3,\, 1$, respectively.

JHEP11(2015)067

C Fragmentation functions for Λ_b and Λ_c

In this appendix we express the polarization retention factors r_L and r_T defined in eq. (1.1) in terms of the $b \to \Lambda_b$ fragmentation functions. In particular, we want to show that

$$r_L(z) = \frac{G_1(z)}{D_1(z)}\,, \qquad r_T(z) = \frac{H_1(z)}{D_1(z)}\,, \tag{C.1}$$

where z is the fraction of the initial b-quark momentum carried by the Λ_b, and the fragmentation functions $G_1(z), H_1(z), D_1(z)$ are defined below (see also ref. [123]). These can then be used to compute how r_L and r_T vary with the scale of the hard process. The same formalism applies to $c \to \Lambda_c$ fragmentation functions.

The cross section for a hadron h with transverse momentum p_T and spin state S_h is given by, see e.g., ref. [31],

$$\frac{d\sigma\,(pp \to h(S_h) + X + \ldots)}{dp_T} = \int d\hat{p}_T dz \sum_q \mathrm{Tr}\left[\frac{d\hat{\sigma}\,(pp \to q + \ldots)}{d\hat{p}_T}\Delta_q^h(S_h, z)\right]\delta(p_T - z\hat{p}_T), \tag{C.2}$$

where $d\hat{\sigma}/d\hat{p}_T$ is the differential cross section for production of the hard parton q, without fragmentation, in the process of interest, X denotes the additional particles produced in the fragmentation of q, and ellipses denote all the other final-state particles. We have suppressed the dependence on the factorization scale μ of both $d\hat{\sigma}/d\hat{p}_T$ and Δ_q^h, the latter containing the fragmentation functions. The fragmentation functions are universal, independent of the hard process. The trace in eq. (C.2) contracts the Dirac indices of the outgoing q in $d\hat{\sigma}/d\hat{p}_T$ with those of Δ_q^h. We are interested in the case $q = b$, $h = \Lambda_b$ and, separately, also in the case $q = c$, $h = \Lambda_c$.

In the ultra-relativistic limit, for a quark q with momentum k hadronizing to a spin-1/2 hadron h with mass M_h, momentum P_h and spin S_h, the relevant fragmentation functions $D_1(z)$, $G_1(z)$, and $H_1(z)$ are given by (see, e.g., refs. [38, 123–126])

$$\Delta_q^h(S_h, z) = \sum_X \int \frac{z\,d\xi^+ d^2\vec{\xi}_T d^2\vec{k}_T}{2(2\pi)^3} e^{ik\cdot\xi}\langle 0|q(\xi)|X; P_h, S_h\rangle\langle X; P_h, S_h|\bar{q}(0)|0\rangle\Big|_{\xi^-=0}\,, \tag{C.3}$$

where

$$\Delta_q^h(S_h, z) = \frac{1}{2}\Big(D_1(z)\,\not{n}_- + G_1(z)\,\lambda_h\gamma_5\,\not{n}_- + H_1(z)\,i\sigma_{\mu\nu}\gamma_5 n_-^\mu S_{hT}^\nu/M_h\Big)\,, \tag{C.4}$$

where we use light-cone coordinates with $n_\pm^\mu = (1, 0, 0, \pm 1)$ and take n_- to be aligned with k. The light-cone components of a four-vector are $a^\pm \equiv a \cdot n_\mp$. We also use $z = P_h^-/k^-$ as the light-cone fraction of the quark momentum carried by the hadron h and the sum is over all the hadronic states X that accompany h in the jet. S_h^μ is the spin vector describing a pure spin-1/2 state, which in the rest frame of the hadron is just $S_h^\mu = M_h\,(0, \vec{s}_h)$ (see, e.g., ref. [127]). It has been expressed above in terms of the light-cone helicity $\lambda_h = S_h^-/P_h^-$ and the transverse components $S_{hT}^\mu = S_h^\mu - S_h^- n_-^\mu/2 + (S_h^- M_h^2/P_h^{-2})\,n_+^\mu/2$.

The fragmentation function $D_1(z)$ describes the probability for a certain hadron to be produced from a given quark. The total *fragmentation fraction*, like the ones quoted in

JHEP11(2015)067

eqs. (2.2) and (2.3), is then given by

$$f_{q\to h} = \int_0^1 dz\, D^h_{1,q}(z). \tag{C.5}$$

The fragmentation functions $G_1(z)$ and $H_1(z)$ encode, in addition, the polarization of the hadron when produced from a quark with spin pointing in longitudinal and transverse direction, respectively [123, 128]. We have suppressed the h, q indices on the fragmentation functions in eq. (C.4) and the fact that they depend on the factorization scale μ.

For heavy quarks some control on the fragmentation functions can be achieved using HQET, see e.g. refs. [129–132]. This is relevant for the polarization of Λ_b as the main depolarization effect indeed originates from the finite quark mass and can thus be described in HQET. In the exact $m_b \to \infty$ limit, the Λ_b spin is completely aligned with the spin of the b quark. Therefore, the product of matrix elements in eq. (C.3) has the same Lorentz structure as the outer product of the two b-quark Dirac spinors

$$u_b\bar{u}_b = m_b \frac{1+\not{v}_b}{2}\left(1+\gamma_5\frac{\not{S}_b}{m_b}\right) = m_b\frac{1+\not{v}_b}{2}\left(1-\frac{S_b\cdot\epsilon_3^b}{m_b}\,\gamma_5\not{\epsilon}_3^b+\gamma_5\frac{\not{S}_{bT}}{m_b}\right). \tag{C.6}$$

Here, v_b^μ and $\epsilon_3^{b\,\mu}$ coincide with the hadron velocity four-vector, $v^\mu \equiv P_h^\mu/M_h = (E_h, 0, 0, p_h)/M_h$, (where in our conventions $p_h < 0$) and its longitudinal polarization vector, $\epsilon_3^\mu = (p_h, 0, 0, E_h)/M_h$, respectively. They satisfy $v^2 = 1$, $\epsilon_3^2 = -1$, $v\cdot\epsilon_3 = 0$, and $v\cdot S_h = 0$. In this formal limit the fragmentation function of a heavy b quark to $h = \Lambda_b$ reads

$$\Delta_b^h(S_h, z) = \frac{2M_h}{E_h - p_h}\frac{1+\not{v}}{2}\left(D_1(z) - G_1(z)\frac{S_h\cdot\epsilon_3}{M_h}\gamma_5\not{\epsilon}_3 + H_1(z)\gamma_5\frac{\not{S}_{hT}}{M_h}\right), \tag{C.7}$$

with

$$D_1(z) = G_1(z) = H_1(z) \propto \delta(1-z)\,. \tag{C.8}$$

We see that in the heavy-quark limit, the Λ_b fragmentation functions at $\mu \lesssim m_b$ are given by a single function. Eqs. (C.4) and (C.7) coincide in the ultra-relativistic limit in which $v^\mu = n_-^\mu E_h/M_h + \cdots$, $\epsilon_3^\mu = v^\mu - n_+^\mu M_h/2E_h + \cdots$. Apart from RG effects discussed below, measurements with highly energetic jets thus probe deviations from eq. (C.8), which are precisely the finite-m_b effects calculable in HQET. A perturbative treatment of heavy-quark fragmentation is possible, if the fragmentation function is summed over all possible final states [129]; for the nonperturbative endpoint region $z \sim 1$ see ref. [131]. We restrict ourselves to the exclusive case of fragmenting to one heavy hadron and make no assumptions about the form of the fragmentation functions. Unpolarized fragmentation functions, $D_1(z)$, have been measured for inclusive samples of b hadrons at LEP [67–69] and SLD [70], and for the Λ_c by CLEO [133], Belle [134] and BaBar [135]. See refs. [131, 136] for theoretical interpretations of such measurements. No measurements of polarized fragmentation functions are available yet.

As argued in the main part of the paper, when departing from the heavy-quark limit the dominant effect of depolarization is due to the hadronization of the b quark into not only

JHEP11(2015)067

Λ_b but also into Σ_b and Σ_b^* baryons. The $\Sigma_b^{(*)}$'s decay to Λ_b via strong interactions, albeit with a phase-space suppressed decay width that parametrically enhances the depolarization effect. We have parameterized the relative production probabilities of the Λ_b and $\Sigma_b^{(*)}$ states using the nonperturbative parameters w_1 and A from eq. (2.7) and in the narrow-width limit R from eq. (3.9), to compute the polarization retention factors r_L and r_T. They are directly related to the fragmentation functions

$$r_L(z) = \frac{G_1(z)}{D_1(z)}\,, \qquad r_T(z) = \frac{H_1(z)}{D_1(z)}\,, \tag{C.9}$$

which are the two relations already advertised in eq. (C.1). The two relations can be easily understood from eq. (C.4) or (C.7). For instance, the longitudinal spin projector will select the $D_1 \pm G_1$ combination for positively (negatively) longitudinally polarized baryon, while H_1 is similarly related to transverse baryon spin.

For example, suppose that a P_L (P_R) projector in the hard kernel acts on the outgoing b quark, so that a left-handed (right-handed) b quark is produced. If we measure the spin of the Λ_b along its direction of motion, this projector gets multiplied by the linear combination $D_1 \mp \gamma_5 G_1$ of the fragmentation functions in eq. (C.4). In the case that $D_1 = G_1$ — like in the heavy-quark limit — the fragmentation function itself is proportional to the same projector; thus a fully longitudinally polarized Λ_b with negative (positive) helicity is produced after the fragmentation, i.e. $r_L(z) = 1$, compatible with eq. (C.9). Oppositely, if $G_1(z) = 0$ and $H_1(z) = 0$, the probability of producing a Λ_b of specific spin S_{Λ_b} would be independent of the underlying spin of the b quark; this is possible only if the polarization is lost completely, i.e. $r_{L,T}(z) = 0$.

Now we would like to explain several points using the example of Λ_b production in e^+e^- collisions at a specific center-of-mass energy, $E_{\rm cm}$. The cross section for producing a Λ_b with spin S_h is given by the usual convolution of hard kernels with fragmentation functions [131]

$$\frac{d\sigma_{\Lambda_b}(S_h)}{dz}(e^+e^- \to \Lambda_b + X) = \sum_i \int_z^1 \frac{dx}{x} \mathrm{Tr}\big[\mathcal{H}_i(E_{\rm cm}, x, \mu)\Delta_i^{\Lambda_b}(S_h, z/x, \mu)\big]\,. \tag{C.10}$$

Here, $\mathcal{H}_i$ are the perturbatively calculable hard kernels, z and x the fractions of the total available energy carried by the Λ_b and the initial parton i, respectively, and the sum is over all final-state partons. In principle one may worry about subleading corrections due to Λ_b fragmenting from an initial gluon or light quark. These corrections are process dependent and are practically negligible for the processes we are interested in. As an example consider Λ_b production on the Z pole, which is dominated by the $e^+e^- \to Z \to b\bar{b}$ partonic process. The longitudinal polarization retention fraction is given by

$$r_L(z) = \frac{G_{1,b}^{\Lambda_b}(z) + \sum_i G_{1,i}^{\Lambda_b}(z)\big(\sigma_L^i - \sigma_R^i\big)/\big(\sigma_L^b - \sigma_R^b\big)}{D_{1,b}^{\Lambda_b}(z) + \sum_i D_{1,i}^{\Lambda_b}(z)\big(\sigma_L^i + \sigma_R^i\big)/\big(\sigma_L^b + \sigma_R^b\big)}\,, \tag{C.11}$$

where the $\sigma_{L,R}^b$ are the partonic cross sections for the left-(right-)handed b quark, and similarly for the other partons $i = u, \bar{u}, d, \bar{d}, \ldots$. Here we see a small violation of universality

JHEP11(2015)067

not due to the scale dependence but due to the sum over light quarks and anti-quarks in eq. (C.11). These non-universal contributions are suppressed by $\alpha_s^2(m_b)$ as they require fragmentation of a light quark (or antiquark) to a heavy-quark baryon, $D_{1,i}^{\Lambda_b}(z)$, $G_{1,i}^{\Lambda_b}(z)$, and are thus small (such perturbative fragmentation was calculated in ref. [137]). For Z decays, the fraction of events containing $g \to b\bar{b}$ (or $g \to c\bar{c}$) is only about 0.3% (3%), as determined both theoretically and experimentally (see table 17.2 of ref. [51]). These numbers still need to be multiplied by the relative branching fraction of the total $q\bar{q}$ vs. $b\bar{b}$.

The next point we would like to make is that in the main text, r_L and r_T describe the average properties of the full sample, which includes baryons with all the possible values of z. Thus, the retention factors are, for fixed center of mass as in the above example of Z pole or for t decays, given by

$$r_L = \frac{\int_0^1 dz\, G_1(z)}{\int_0^1 dz\, D_1(z)}\,, \qquad r_T = \frac{\int_0^1 dz\, H_1(z)}{\int_0^1 dz\, D_1(z)}\,. \tag{C.12}$$

Just like the fragmentation functions, they are independent of the production process, except for a logarithmic dependence on the hard scale. In the example of eq. (C.10) integration over all possible z for $i = b$ leads to

$$\sigma(S_{\Lambda_b}) = \mathrm{Tr} \int_0^1 dx\, \mathcal{H}_b(E_{\rm cm}, x, \mu) \int_0^1 dz\, \Delta_b^{\Lambda_b}(S_{\Lambda_b}, z, \mu)\,. \tag{C.13}$$

This demonstrates explicitly that as long as we are only interested in the polarization from Λ_b's of all z's only the inclusive retention factors are needed.

The polarization retention factors r_L and r_T are universal, up to the logarithmic running of the fragmentation functions with the characteristic energy scale of the process. Therefore the universality violations will be small if they are used for new physics measurements at scales not too different from the scale at which $r_{L,T}$, or equivalently D_1, G_1, and H_1, are first extracted (e.g., r_L in top decays as we propose in this paper). The fragmentation functions evolution is governed by perturbative splitting functions, similarly to the evolution of parton distribution functions (see, e.g., refs. [138, 139]). The resulting universality violations can be estimated for instance using the model for the fragmentation functions in ref. [38], with the LO RG running calculated in ref. [140] (see also refs. [123, 139]), in which the violation in $r_{L,T}$ universality is seen to be relatively mild. Taking the results of ref. [38] at face value the r_T is found to change by $\mathcal{O}(15\%)$ due to the RG running between 5 GeV and 45 GeV for Λ_b (and by $\mathcal{O}(10\%)$ for Λ_c due to running from 2.2 GeV to 45 GeV), while the change in r_L is $\mathcal{O}(5\%)$ ($\mathcal{O}(15\%)$ for Λ_c). We stress that these estimates apply only to the model of fragmentation functions as obtained in ref. [38], and could differ for the measured (in the future) shapes of fragmentation functions.

Once sufficiently precise measurements of $r_{L,T}(z)$ are available, it will be possible to extract the fragmentation functions from them (using also information on unpolarized b-hadron production). The Λ_b production cross section and polarization retention in new physics models can then be calculated using factorization expressions as in eqs. (C.2) and (C.10) after evolving the fragmentation functions to the relevant scale.

JHEP11(2015)067

Finally, we would like to comment on the experimental analyses [23, 27–30, 141], mentioned in section 2, which measured the p_T dependence of the ratios of fragmentation fractions for different b hadrons. Using eq. (C.2), restricting to $q = b$, the differential cross section for the production of an unpolarized b hadron is given by

$$\frac{d\sigma^h}{dp_T^h} = \int_0^1 \frac{dz}{z} \left.\frac{d\hat{\sigma}^b}{d\hat{p}_T^b}\right|_{\hat{p}_T^b = p_T^h/z} D_{1,b}^h(z)\,. \tag{C.14}$$

The experiments report p_T dependences of the fragmentation fraction ratios, which are thus given by

$$\frac{f_{b\to h_1}(p_T^h)}{f_{b\to h_2}(p_T^h)} = \frac{\displaystyle\int_0^1 \frac{dz}{z} \left.\frac{d\hat{\sigma}^b}{d\hat{p}_T^b}\right|_{\hat{p}_T^b = p_T^h/z} D_{1,b}^{h_1}(z)}{\displaystyle\int_0^1 \frac{dz}{z} \left.\frac{d\hat{\sigma}^b}{d\hat{p}_T^b}\right|_{\hat{p}_T^b = p_T^h/z} D_{1,b}^{h_2}(z)}\,. \tag{C.15}$$

We note that the dependence on the details of the hard process does not cancel out, as long as $D_{1,b}^{h_1}(z)$ is not proportional $D_{1,b}^{h_2}(z)$, therefore these ratios are not universal quantities. To extract the fragmentation functions, $D_{1,b}^h(z)$, and the fragmentation fractions, eq. (C.5), it would be useful to measure cross sections differential in two variables, in bins of both the reconstructed b-quark p_T and the reconstructed b-quark momentum fraction carried by the Λ_b. The reconstructed b-quark momentum is obtained by adding to the b-jet momentum the momenta of neutrinos.

References

[1] CMS collaboration, *Measurement of top quark polarization in t-channel single-top production*, CMS-PAS-TOP-13-001 (2013).

[2] J.A. Aguilar-Saavedra and S. Amor dos Santos, *New directions for top quark polarization in the t-channel process*, *Phys. Rev.* **D 89** (2014) 114009 [arXiv:1404.1585] [INSPIRE].

[3] R. Harnik, A. Martin, T. Okui, R. Primulando and F. Yu, *Measuring CP-violation in $h \to \tau^+\tau^-$ at colliders*, *Phys. Rev.* **D 88** (2013) 076009 [arXiv:1308.1094] [INSPIRE].

[4] M. Blanke, G.F. Giudice, P. Paradisi, G. Perez and J. Zupan, *Flavoured naturalness*, *JHEP* **06** (2013) 022 [arXiv:1302.7232] [INSPIRE].

[5] I. Galon, G. Perez and Y. Shadmi, *Non-degenerate squarks from flavored gauge mediation*, *JHEP* **09** (2013) 117 [arXiv:1306.6631] [INSPIRE].

[6] B. Keren-Zur et al., *On partial compositeness and the CP asymmetry in charm decays*, *Nucl. Phys.* **B 867** (2013) 394 [arXiv:1205.5803] [INSPIRE].

[7] C. Delaunay et al., *Light non-degenerate composite partners at the LHC*, *JHEP* **02** (2014) 055 [arXiv:1311.2072] [INSPIRE].

JHEP11(2015)067

[8] S. Fichet, B. Herrmann and Y. Stoll, *Tasting the* SU(5) *nature of supersymmetry at the LHC*, *JHEP* **05** (2015) 091 [arXiv:1501.05307] [INSPIRE].

[9] T. Mannel and G.A. Schuler, *Semileptonic decays of bottom baryons at LEP*, *Phys. Lett.* **B 279** (1992) 194 [INSPIRE].

[10] A.H. Ball et al., *Report of the b fragmentation working group*, *J. Phys.* **G 18** (1992) 1703 [INSPIRE].

[11] A.F. Falk and M.E. Peskin, *Production, decay and polarization of excited heavy hadrons*, *Phys. Rev.* **D 49** (1994) 3320 [hep-ph/9308241] [INSPIRE].

[12] ALEPH collaboration, D. Buskulic et al., *Measurement of Λ_b polarization in Z decays*, *Phys. Lett.* **B 365** (1996) 437 [INSPIRE].

[13] OPAL collaboration, G. Abbiendi et al., *Measurement of the average polarization of b baryons in hadronic Z^0 decays*, *Phys. Lett.* **B 444** (1998) 539 [hep-ex/9808006] [INSPIRE].

[14] DELPHI collaboration, P. Abreu et al., *Λ_b polarization in Z^0 decays at LEP*, *Phys. Lett.* **B 474** (2000) 205 [INSPIRE].

[15] ATLAS collaboration, *Measurement of the cross section of high transverse momentum $Z \to b\bar{b}$ production in proton-proton collisions at $\sqrt{s} = 8TeV$ with the ATLAS detector*, *Phys. Lett.* **B 738** (2014) 25 [arXiv:1404.7042] [INSPIRE].

[16] W.G.D. Dharmaratna and G.R. Goldstein, *Single quark polarization in quantum chromodynamics subprocesses*, *Phys. Rev.* **D 53** (1996) 1073 [INSPIRE].

[17] LHCb collaboration, *Measurements of the $\Lambda_b^0 \to J/\psi\Lambda$ decay amplitudes and the Λ_b^0 polarisation in pp collisions at $\sqrt{s} = 7$ TeV*, *Phys. Lett.* **B 724** (2013) 27 [arXiv:1302.5578] [INSPIRE].

[18] ATLAS collaboration, *Measurement of the parity-violating asymmetry parameter α_b and the helicity amplitudes for the decay $\Lambda_b^0 \to J/\psi + \Lambda^0$ with the ATLAS detector*, *Phys. Rev.* **D 89** (2014) 092009 [arXiv:1404.1071] [INSPIRE].

[19] M. Ivova Rikova, *Measurement of the Λ_b Polarization with pp collisions at 7 TeV*, CERN-THESIS-2013-218 (2013).

[20] M. Jezabek, K. Rybicki and R. Rylko, *Experimental study of spin effects in hadroproduction and decay of Λ_c^+*, *Phys. Lett.* **B 286** (1992) 175 [INSPIRE].

[21] E791 collaboration, E.M. Aitala et al., *Multidimensional resonance analysis of $\Lambda_c^+ \to pK^-\pi^+$*, *Phys. Lett.* **B 471** (2000) 449 [hep-ex/9912003] [INSPIRE].

[22] J.G. Korner, M. Krämer and D. Pirjol, *Heavy baryons*, *Prog. Part. Nucl. Phys.* **33** (1994) 787 [hep-ph/9406359] [INSPIRE].

[23] Heavy Flavor Averaging Group (HFAG) collaboration, Y. Amhis et al., *Averages of b-hadron, c-hadron and τ-lepton properties as of summer 2014*, arXiv:1412.7515 [INSPIRE].

[24] CDF collaboration, T. Aaltonen et al., *Observation of the Ω_b^- and measurement of the properties of the Ξ_b^- and Ω_b^-*, *Phys. Rev.* **D 80** (2009) 072003 [arXiv:0905.3123] [INSPIRE].

[25] H.-Y. Cheng, *Nonleptonic weak decays of bottom baryons*, *Phys. Rev.* **D 56** (1997) 2799 [hep-ph/9612223] [INSPIRE].

[26] L. Gladilin, *Fragmentation fractions of c and b quarks into charmed hadrons at LEP*, *Eur. Phys. J.* **C 75** (2015) 19 [arXiv:1404.3888] [INSPIRE].

JHEP11(2015)067

[27] CDF collaboration, T. Aaltonen et al., *First measurement of the ratio of branching fractions* $B(\Lambda_b^0 \to \Lambda_c^+ \mu^- \bar{\nu}_\mu)/B(\Lambda_b^0 \to \Lambda_c^+ \pi^-)$, *Phys. Rev.* **D 79** (2009) 032001 [arXiv:0810.3213] [INSPIRE].

[28] CMS collaboration, *Measurement of the* Λ_b *cross section and the* $\bar{\Lambda}_b$ *to* Λ_b *ratio with* $J/\psi\Lambda$ *decays in pp collisions at* $\sqrt{s} = 7$ *TeV*, *Phys. Lett.* **B 714** (2013) 136 [arXiv:1205.0594] [INSPIRE].

[29] LHCb collaboration, *Measurement of b-hadron production fractions in 7 TeV pp collisions*, *Phys. Rev.* **D 85** (2012) 032008 [arXiv:1111.2357] [INSPIRE].

[30] LHCb collaboration, *Study of the kinematic dependences of* Λ_b^0 *production in pp collisions and a measurement of the* $\Lambda_b^0 \to \Lambda_c^+ \pi^-$ *branching fraction*, *JHEP* **08** (2014) 143 [arXiv:1405.6842] [INSPIRE].

[31] M. Cacciari and P. Nason, *Is there a significant excess in bottom hadroproduction at the Tevatron?*, *Phys. Rev. Lett.* **89** (2002) 122003 [hep-ph/0204025] [INSPIRE].

[32] CDF collaboration, T. Aaltonen et al., *First observation of heavy baryons* Σ_b *and* Σ_b^*, *Phys. Rev. Lett.* **99** (2007) 202001 [arXiv:0706.3868] [INSPIRE].

[33] CDF collaboration, T. Aaltonen et al., *Measurement of the masses and widths of the bottom baryons* $\Sigma_b^\pm$ *and* $\Sigma_b^{*\pm}$, *Phys. Rev.* **D 85** (2012) 092011 [arXiv:1112.2808] [INSPIRE].

[34] A. Andronic, F. Beutler, P. Braun-Munzinger, K. Redlich and J. Stachel, *Statistical hadronization of heavy flavor quarks in elementary collisions: Successes and failures*, *Phys. Lett.* **B 678** (2009) 350 [arXiv:0904.1368] [INSPIRE].

[35] T. Sjöstrand, S. Mrenna and P.Z. Skands, *PYTHIA 6.4 physics and manual*, *JHEP* **05** (2006) 026 [hep-ph/0603175] [INSPIRE].

[36] P.Z. Skands, *Tuning Monte Carlo generators: the Perugia tunes*, *Phys. Rev.* **D 82** (2010) 074018 [arXiv:1005.3457] [INSPIRE].

[37] P. Skands, S. Carrazza and J. Rojo, *Tuning PYTHIA 8.1: the Monash 2013 tune*, *Eur. Phys. J.* **C 74** (2014) 3024 [arXiv:1404.5630] [INSPIRE].

[38] A. Adamov and G.R. Goldstein, *Excited state contributions to the heavy baryon fragmentation functions in a quark-diquark model*, *Phys. Rev.* **D 64** (2001) 014021 [hep-ph/0009300] [INSPIRE].

[39] E791 collaboration, E.M. Aitala et al., *Mass splitting and production of* Σ_c^0 *and* Σ_c^{++} *measured in 500 GeV* π^-*-N interactions*, *Phys. Lett.* **B 379** (1996) 292 [hep-ex/9604007] [INSPIRE].

[40] DELPHI collaboration, M. Feindt et al., *First evidence for* Σ_b *and* Σ_b^* *baryons*, DELPHI-95-107 (1995).

[41] M. Feindt, *Heavy quark spectroscopy at LEP*, CERN-PPE-95-139 (1995).

[42] O. Podobrin, *B-hadron production at LEP*, *Nucl. Phys. Proc. Suppl.* **50** (1996) 90.

[43] CLEO collaboration, G. Brandenburg et al., *Observation of two excited charmed baryons decaying into* $\Lambda_c^+ \pi^\pm$, *Phys. Rev. Lett.* **78** (1997) 2304 [INSPIRE].

[44] Y.-Q. Chen and M.B. Wise, *Remark on charm quark fragmentation to* D^{**} *mesons*, *Phys. Rev.* **D 50** (1994) 4706 [hep-ph/9404240] [INSPIRE].

[45] T.C. Yuan, *Helicity probabilities for heavy quark fragmentation into excited mesons*, *Phys. Rev.* **D 51** (1995) 4830 [hep-ph/9407341] [INSPIRE].

JHEP11(2015)067

[46] J.K. Elwood, *Excited charmed baryon decays and their implications for fragmentation parameters*, *Phys. Rev.* **D 53** (1996) 4866 [hep-ph/9511241] [INSPIRE].

[47] C.-K. Chow, *Qualitative aspects of polarization distributions in excited heavy hadron productions*, hep-ph/9609514 [INSPIRE].

[48] J.P. Ma, *Revisiting spin alignment of heavy mesons in its inclusive production*, *Nucl. Phys.* **B 622** (2002) 416 [hep-ph/0111237] [INSPIRE].

[49] BELLE collaboration, V. Balagura et al., *Observation of $D_{s1}(2536)^+ \to D^+\pi^-K^+$ and angular decomposition of $D_{s1}(2536)^+ \to D^{*+}K^0_S$*, *Phys. Rev.* **D 77** (2008) 032001 [arXiv:0709.4184] [INSPIRE].

[50] J.G. Korner, A. Pilaftsis and M.M. Tung, *One loop QCD mass effects in the production of polarized bottom and top quarks*, *Z. Phys.* **C 63** (1994) 575 [hep-ph/9311332] [INSPIRE].

[51] PARTICLE DATA GROUP collaboration, K.A. Olive et al., *Review of particle physics*, *Chin. Phys.* **C 38** (2014) 090001 [INSPIRE].

[52] M. Baumgart and B. Tweedie, *Transverse top quark polarization and the $t\bar{t}$ forward-backward asymmetry*, *JHEP* **08** (2013) 072 [arXiv:1303.1200] [INSPIRE].

[53] ALICE collaboration, *Measurement of charm production at central rapidity in proton-proton collisions at $\sqrt{s} = 2.76$ TeV*, *JHEP* **07** (2012) 191 [arXiv:1205.4007] [INSPIRE].

[54] CLEO collaboration, G. Brandenburg et al., *Continuum charged D^* spin alignment at $\sqrt{s} = 10.5$ GeV*, *Phys. Rev.* **D 58** (1998) 052003 [hep-ex/9802022] [INSPIRE].

[55] T.-M. Yan, H.-Y. Cheng, C.-Y. Cheung, G.-L. Lin, Y.C. Lin and H.-L. Yu, *Heavy quark symmetry and chiral dynamics*, *Phys. Rev.* **D 46** (1992) 1148 [*Erratum ibid.* **D 55** (1997) 5851] [INSPIRE].

[56] G. Bonvicini and L. Randall, *Optimized variables for the study of Λ_b polarization*, *Phys. Rev. Lett.* **73** (1994) 392 [hep-ph/9401299] [INSPIRE].

[57] B. Mele, *Lepton spectra and the b polarization at LEP*, *Mod. Phys. Lett.* **A 9** (1994) 1239 [hep-ph/9403302] [INSPIRE].

[58] ALEPH collaboration, D. Buskulic et al., *Measurement of Λ polarization from Z decays*, *Phys. Lett.* **B 374** (1996) 319 [INSPIRE].

[59] ALEPH collaboration, *Update of Λ polarization from Z decays*, CERN-OPEN-99-328 (1997).

[60] OPAL collaboration, K. Ackerstaff et al., *Polarization and forward-backward asymmetry of Λ baryons in hadronic Z^0 decays*, *Eur. Phys. J.* **C 2** (1998) 49 [hep-ex/9708027] [INSPIRE].

[61] G.R. Goldstein, *Polarization of inclusively produced Λ_c in a QCD based hybrid model*, hep-ph/9907573 [INSPIRE].

[62] A.V. Manohar and M.B. Wise, *Inclusive semileptonic B and polarized Λ_b decays from QCD*, *Phys. Rev.* **D 49** (1994) 1310 [hep-ph/9308246] [INSPIRE].

[63] A. Czarnecki, M. Jezabek, J.G. Korner and J.H. Kuhn, *QCD corrections to decays of polarized charm and bottom quarks*, *Phys. Rev. Lett.* **73** (1994) 384 [hep-ph/9312249] [INSPIRE].

[64] A. Czarnecki and M. Jezabek, *Distributions of leptons in decays of polarized heavy quarks*, *Nucl. Phys.* **B 427** (1994) 3 [hep-ph/9402326] [INSPIRE].

JHEP11(2015)067

[65] CMS collaboration, *Algorithms for b jet identification in CMS*, CMS-PAS-BTV-09-001 (2009).

[66] LHCb collaboration, *Precision measurement of the ratio of the Λ_b^0 to $\overline{B}^0$ lifetimes*, *Phys. Lett.* **B 734** (2014) 122 [arXiv:1402.6242] [INSPIRE].

[67] ALEPH collaboration, A. Heister et al., *Study of the fragmentation of b quarks into B mesons at the Z peak*, *Phys. Lett.* **B 512** (2001) 30 [hep-ex/0106051] [INSPIRE].

[68] DELPHI collaboration, J. Abdallah et al., *A study of the b-quark fragmentation function with the DELPHI detector at LEP I and an averaged distribution obtained at the Z Pole*, *Eur. Phys. J.* **C 71** (2011) 1557 [arXiv:1102.4748] [INSPIRE].

[69] OPAL collaboration, G. Abbiendi et al., *Inclusive analysis of the b quark fragmentation function in Z decays at LEP*, *Eur. Phys. J.* **C 29** (2003) 463 [hep-ex/0210031] [INSPIRE].

[70] SLD collaboration, K. Abe et al., *Measurement of the b quark fragmentation function in Z^0 decays*, *Phys. Rev.* **D 65** (2002) 092006 [*Erratum ibid.* **D 66** (2002) 079905] [hep-ex/0202031] [INSPIRE].

[71] ATLAS collaboration, *Search for pair-produced third-generation squarks decaying via charm quarks or in compressed supersymmetric scenarios in pp collisions at $\sqrt{s} = 8$ TeV with the ATLAS detector*, *Phys. Rev.* **D 90** (2014) 052008 [arXiv:1407.0608] [INSPIRE].

[72] ATLAS collaboration, *Search for scalar charm quark pair production in pp collisions at $\sqrt{s} = 8$ TeV with the ATLAS detector*, *Phys. Rev. Lett.* **114** (2015) 161801 [arXiv:1501.01325] [INSPIRE].

[73] D0 collaboration, V.M. Abazov et al., *Measurement of the Λ_b^0 lifetime using semileptonic decays*, *Phys. Rev. Lett.* **99** (2007) 182001 [arXiv:0706.2358] [INSPIRE].

[74] O. Gedalia et al., *Top B physics at the LHC*, *Phys. Rev. Lett.* **110** (2013) 232002 [arXiv:1212.4611] [INSPIRE].

[75] CMS collaboration, *Description and performance of track and primary-vertex reconstruction with the CMS tracker*, 2014 *JINST* **9** P10009 [arXiv:1405.6569] [INSPIRE].

[76] BELLE collaboration, A. Zupanc et al., *Measurement of the branching fraction $\mathcal{B}(\Lambda_c^+ \to pK^-\pi^+)$*, *Phys. Rev. Lett.* **113** (2014) 042002 [arXiv:1312.7826] [INSPIRE].

[77] CMS collaboration, *Measurement of the B^+ production cross section in pp collisions at $\sqrt{s} = 7$ TeV*, *Phys. Rev. Lett.* **106** (2011) 112001 [arXiv:1101.0131] [INSPIRE].

[78] CMS collaboration, *Measurement of the B_s^0 production cross section with $B_s^0 \to J/\psi\ \phi$ decays in pp collisions at $\sqrt{s} = 7$ TeV*, *Phys. Rev.* **D 84** (2011) 052008 [arXiv:1106.4048] [INSPIRE].

[79] CMS collaboration, *Measurement of associated W + charm production in pp collisions at $\sqrt{s} = 7$ TeV*, *JHEP* **02** (2014) 013 [arXiv:1310.1138] [INSPIRE].

[80] ATLAS collaboration, *Measurement of the production of a W boson in association with a charm quark in pp collisions at $\sqrt{s} = 7$ TeV with the ATLAS detector*, *JHEP* **05** (2014) 068 [arXiv:1402.6263] [INSPIRE].

[81] S. Dambach, U. Langenegger and A. Starodumov, *Neutrino reconstruction with topological information*, *Nucl. Instrum. Meth.* **A 569** (2006) 824 [hep-ph/0607294] [INSPIRE].

[82] LHCb collaboration, *Determination of the quark coupling strength $|V_{ub}|$ using baryonic decays*, *Nature Phys.* **11** (2015) 743 [arXiv:1504.01568] [INSPIRE].

JHEP11(2015)067

[83] CMS collaboration, *Measurement of the top quark mass using the B-hadron lifetime technique*, CMS-PAS-TOP-12-030 (2013).

[84] M. Czakon and A. Mitov, *Top++: a program for the calculation of the top-pair cross-section at hadron colliders*, *Comput. Phys. Commun.* **185** (2014) 2930 [arXiv:1112.5675] [INSPIRE].

[85] R. Gavin, Y. Li, F. Petriello and S. Quackenbush, *FEWZ 2.0: a code for hadronic Z production at next-to-next-to-leading order*, *Comput. Phys. Commun.* **182** (2011) 2388 [arXiv:1011.3540] [INSPIRE].

[86] Y. Li and F. Petriello, *Combining QCD and electroweak corrections to dilepton production in FEWZ*, *Phys. Rev.* **D 86** (2012) 094034 [arXiv:1208.5967] [INSPIRE].

[87] P. Kant et al., *HatHor for single top-quark production: updated predictions and uncertainty estimates for single top-quark production in hadronic collisions*, *Comput. Phys. Commun.* **191** (2015) 74 [arXiv:1406.4403] [INSPIRE].

[88] J. Alwall, M. Herquet, F. Maltoni, O. Mattelaer and T. Stelzer, *MadGraph 5: going beyond*, *JHEP* **06** (2011) 128 [arXiv:1106.0522] [INSPIRE].

[89] J. D'Hondt et al., *Fitting of event topologies with external kinematic constraints in CMS*, CMS-NOTE-2006-023 (2006).

[90] J. Erdmann et al., *A likelihood-based reconstruction algorithm for top-quark pairs and the KLFitter framework*, *Nucl. Instrum. Meth.* **A 748** (2014) 18 [arXiv:1312.5595] [INSPIRE].

[91] B.A. Betchart, R. Demina and A. Harel, *Analytic solutions for neutrino momenta in decay of top quarks*, *Nucl. Instrum. Meth.* **A 736** (2014) 169 [arXiv:1305.1878] [INSPIRE].

[92] ATLAS collaboration, *Measurements of normalized differential cross sections for $t\bar{t}$ production in pp collisions at $\sqrt{s} = 7$ TeV using the ATLAS detector*, *Phys. Rev.* **D 90** (2014) 072004 [arXiv:1407.0371] [INSPIRE].

[93] CMS collaboration, *Measurement of the differential cross section for top quark pair production in pp collisions at $\sqrt{s} = 8$ TeV*, arXiv:1505.04480 [INSPIRE].

[94] CMS collaboration, *Measurement of the inclusive and differential $t\bar{t}$ production cross sections in lepton + jets final states at 13 TeV*, CMS-PAS-TOP-15-005 (2015).

[95] CMS collaboration, *Measurement of the t-channel single top quark production cross section in pp collisions at $\sqrt{s} = 7$ TeV*, *Phys. Rev. Lett.* **107** (2011) 091802 [arXiv:1106.3052] [INSPIRE].

[96] J.D. Bjorken, *Spin dependent decays of the Λ_c*, *Phys. Rev.* **D 40** (1989) 1513 [INSPIRE].

[97] ATLAS collaboration, *dE/dx measurement in the ATLAS Pixel detector and its use for particle identification*, ATLAS-CONF-2011-016 (2011).

[98] ATLAS collaboration, *Particle identification performance of the ATLAS transition radiation tracker*, ATLAS-CONF-2011-128 (2011).

[99] A. Giammanco, *Particle identification with energy loss in the CMS silicon strip tracker*, CMS-NOTE-2008-005 (2008).

[100] CMS collaboration, *CMS tracking performance results from early LHC operation*, *Eur. Phys. J.* **C 70** (2010) 1165 [arXiv:1007.1988] [INSPIRE].

JHEP11(2015)067

[101] A. Zagoździńska, K. T. Poźniak, R. Romaniuk and P. Zalewski, *Heavy stable charged particles search by RPC system at CMS detector at LHC accelerator at CERN*, *Proc. SPIE* **8903** (2013) 89031K.

[102] CMS collaboration, *Measurement of the top-quark mass in $t\bar{t}$ events with lepton+jets final states in pp collisions at $\sqrt{s} = 8$ TeV*, CMS-PAS-TOP-14-001 (2014).

[103] CMS collaboration, *Identification of b-quark jets with the CMS experiment*, 2013 *JINST* **8** P04013 [arXiv:1211.4462] [INSPIRE].

[104] LHCb collaboration, *Observation of two new Ξ_b^- baryon resonances*, *Phys. Rev. Lett.* **114** (2015) 062004 [arXiv:1411.4849] [INSPIRE].

[105] CMS collaboration, *Observation of a new Ξ_b baryon*, *Phys. Rev. Lett.* **108** (2012) 252002 [arXiv:1204.5955] [INSPIRE].

[106] M.A. Ivanov, J.G. Korner, V.E. Lyubovitskij and A.G. Rusetsky, *Exclusive nonleptonic bottom to charm baryon decays including nonfactorizable contributions*, *Mod. Phys. Lett.* **A 13** (1998) 181 [hep-ph/9709325] [INSPIRE].

[107] M.A. Ivanov, J.G. Korner, V.E. Lyubovitskij and A.G. Rusetsky, *Exclusive nonleptonic decays of bottom and charm baryons in a relativistic three quark model: evaluation of nonfactorizing diagrams*, *Phys. Rev.* **D 57** (1998) 5632 [hep-ph/9709372] [INSPIRE].

[108] J.-P. Lee, C. Liu and H.S. Song, *Analysis of $\Lambda_b \to \Lambda_c$ weak decays in heavy quark effective theory*, *Phys. Rev.* **D 58** (1998) 014013 [hep-ph/9803489] [INSPIRE].

[109] X.H. Guo, *$\Lambda_b \to \Lambda_c P(V)$ nonleptonic weak decays*, *Mod. Phys. Lett.* **A 13** (1998) 2265 [hep-ph/9805304] [INSPIRE].

[110] R. Mohanta, A.K. Giri, M.P. Khanna, M. Ishida, S. Ishida and M. Oda, *Hadronic weak decays of Λ_b baryon in the covariant oscillator quark model*, *Prog. Theor. Phys.* **101** (1999) 959 [hep-ph/9904324] [INSPIRE].

[111] H.-W. Ke, X.-Q. Li and Z.-T. Wei, *Diquarks and $\Lambda_b \to \Lambda_c$ weak decays*, *Phys. Rev.* **D 77** (2008) 014020 [arXiv:0710.1927] [INSPIRE].

[112] T. Gutsche, M.A. Ivanov, J.G. Körner, V.E. Lyubovitskij and P. Santorelli, *Polarization effects in the cascade decay $\Lambda_b \to \Lambda(\to p\pi^-) + J/\psi(\to \ell^+\ell^-)$ in the covariant confined quark model*, *Phys. Rev.* **D 88** (2013) 114018 [arXiv:1309.7879] [INSPIRE].

[113] Fayyazuddin and Riazuddin, *Two-body nonleptonic Λ_b decays in quark model with factorization ansatz*, *Phys. Rev.* **D 58** (1998) 014016 [hep-ph/9802326] [INSPIRE].

[114] C.-H. Chou, H.-H. Shih, S.-C. Lee and H.-n. Li, *$\Lambda_b \to \Lambda J/\psi$ decay in perturbative QCD*, *Phys. Rev.* **D 65** (2002) 074030 [hep-ph/0112145] [INSPIRE].

[115] Z.J. Ajaltouni, E. Conte and O. Leitner, *Λ_b decays into Λ-vector*, *Phys. Lett.* **B 614** (2005) 165 [hep-ph/0412116] [INSPIRE].

[116] Z.-T. Wei, H.-W. Ke and X.-Q. Li, *Evaluating decay rates and asymmetries of Λ_b into light baryons in LFQM*, *Phys. Rev.* **D 80** (2009) 094016 [arXiv:0909.0100] [INSPIRE].

[117] L. Mott and W. Roberts, *Rare dileptonic decays of Λ_b in a quark model*, *Int. J. Mod. Phys.* **A 27** (2012) 1250016 [arXiv:1108.6129] [INSPIRE].

[118] CDF collaboration, T. Aaltonen et al., *Measurements of the properties of $\Lambda_c(2595)$, $\Lambda_c(2625)$, $\Sigma_c(2455)$ and $\Sigma_c(2520)$ baryons*, *Phys. Rev.* **D 84** (2011) 012003 [arXiv:1105.5995] [INSPIRE].

JHEP11(2015)067

[119] Belle collaboration, S.H. Lee et al., *Measurements of the masses and widths of the $\Sigma_c(2455)^{0/++}$ and $\Sigma_c(2520)^{0/++}$ baryons*, *Phys. Rev.* **D 89** (2014) 091102 [arXiv:1404.5389] [INSPIRE].

[120] LHCb collaboration, *Prompt charm production in pp collisions at $\sqrt{s} = 7$ TeV*, *Nucl. Phys.* **B 871** (2013) 1 [arXiv:1302.2864] [INSPIRE].

[121] LHCb collaboration, *Precision measurement of the mass and lifetime of the Ξ_b^- baryon*, *Phys. Rev. Lett.* **113** (2014) 242002 [arXiv:1409.8568] [INSPIRE].

[122] D. Ebert, R.N. Faustov and V.O. Galkin, *Semileptonic decays of heavy baryons in the relativistic quark model*, *Phys. Rev.* **D 73** (2006) 094002 [hep-ph/0604017] [INSPIRE].

[123] V. Barone, A. Drago and P.G. Ratcliffe, *Transverse polarisation of quarks in hadrons*, *Phys. Rept.* **359** (2002) 1 [hep-ph/0104283] [INSPIRE].

[124] D. Boer and P.J. Mulders, *Time reversal odd distribution functions in leptoproduction*, *Phys. Rev.* **D 57** (1998) 5780 [hep-ph/9711485] [INSPIRE].

[125] K. Chen, G.R. Goldstein, R.L. Jaffe and X.-D. Ji, *Probing quark fragmentation functions for spin 1/2 baryon production in unpolarized e^+e^- annihilation*, *Nucl. Phys.* **B 445** (1995) 380 [hep-ph/9410337] [INSPIRE].

[126] R.L. Jaffe and X.-D. Ji, *Novel quark fragmentation functions and the nucleon's transversity distribution*, *Phys. Rev. Lett.* **71** (1993) 2547 [hep-ph/9307329] [INSPIRE].

[127] J. Collins, *Foundations of perturbative QCD*, Cambridge University Press, Cambridge U.K. (2011).

[128] M. Boglione and P.J. Mulders, *Time reversal odd fragmentation and distribution functions in pp and ep single spin asymmetries*, *Phys. Rev.* **D 60** (1999) 054007 [hep-ph/9903354] [INSPIRE].

[129] B. Mele and P. Nason, *The fragmentation function for heavy quarks in QCD*, *Nucl. Phys.* **B 361** (1991) 626 [INSPIRE].

[130] R.L. Jaffe and L. Randall, *Heavy quark fragmentation into heavy mesons*, *Nucl. Phys.* **B 412** (1994) 79 [hep-ph/9306201] [INSPIRE].

[131] M. Neubert, *Factorization analysis for the fragmentation functions of hadrons containing a heavy quark*, arXiv:0706.2136 [INSPIRE].

[132] C.W. Bauer and E. Mereghetti, *Heavy quark fragmenting jet functions*, *JHEP* **04** (2014) 051 [arXiv:1312.5605] [INSPIRE].

[133] CLEO collaboration, P. Avery et al., *Inclusive production of the charmed baryon Λ_c from e^+e^- annihilations at $\sqrt{s} = 10.55$ GeV*, *Phys. Rev.* **D 43** (1991) 3599 [INSPIRE].

[134] Belle collaboration, R. Seuster et al., *Charm hadrons from fragmentation and B decays in e^+e^- annihilation at $\sqrt{s} = 10.6$ GeV*, *Phys. Rev.* **D 73** (2006) 032002 [hep-ex/0506068] [INSPIRE].

[135] BaBar collaboration, B. Aubert et al., *Inclusive Λ_c^+ production in e^+e^- annihilations at $\sqrt{s} = 10.54$ GeV and in $\Upsilon(4S)$ decays*, *Phys. Rev.* **D 75** (2007) 012003 [hep-ex/0609004] [INSPIRE].

[136] M. Cacciari, P. Nason and C. Oleari, *A study of heavy flavored meson fragmentation functions in e^+e^- annihilation*, *JHEP* **04** (2006) 006 [hep-ph/0510032] [INSPIRE].

JHEP11(2015)067

[137] K. Melnikov and A. Mitov, *Perturbative heavy quark fragmentation function through $O(\alpha_s^2)$*, *Phys. Rev.* **D 70** (2004) 034027 [hep-ph/0404143] [INSPIRE].

[138] P. Nason and B.R. Webber, *Scaling violation in e^+e^- fragmentation functions: QCD evolution, hadronization and heavy quark mass effects*, *Nucl. Phys.* **B 421** (1994) 473 [*Erratum ibid.* **B 480** (1996) 755] [INSPIRE].

[139] M. Stratmann and W. Vogelsang, *Next-to-leading order evolution of polarized and unpolarized fragmentation functions*, *Nucl. Phys.* **B 496** (1997) 41 [hep-ph/9612250] [INSPIRE].

[140] X. Artru and M. Mekhfi, *Transversely polarized parton densities, their evolution and their measurement*, *Z. Phys.* **C 45** (1990) 669 [INSPIRE].

[141] LHCb collaboration, *Measurement of the fragmentation fraction ratio f_s/f_d and its dependence on B meson kinematics*, *JHEP* **04** (2013) 001 [arXiv:1301.5286] [INSPIRE].

JHEP11(2015)067